

Unmethylated CpG motif-containing genomic DNA fragment of *Bacillus calmette-guerin* promotes macrophage functions through TLR9-mediated activation of NF- κ B and MAPKs signaling pathways

Innate Immunity
2020, Vol. 26(3) 183–203
© The Author(s) 2019
Article reuse guidelines:
sagepub.com/journals-permissions
DOI: 10.1177/1753425919879997
journals.sagepub.com/home/ini
SAGE

Junli Li^{1,2,3,4,5} , Lili Fu¹, Guozhi Wang¹, Selvakumar Subbian⁶,
Chuan Qin^{2,3,4,5} and Aihua Zhao¹

Abstract

The potency of synthetic CpG-oligo-deoxynucleotides (CpG-ODNs) adjuvants in modulating the immune cell functions through the TLR pathway has been tested and reported previously. However, the cellular signaling involved in the stimulation of macrophages by natural, CpG motif-containing adjuvant and the effector functions modulated by such stimulation has not been well studied. Here, we used *in vitro* and *ex vivo* murine macrophage assay systems, and mouse model of *in vivo* stimulation to explore the signaling pathway and the effector functions mediated by BC01. Results show that BC01 can induce the production of TNF- α and MCP-1 in macrophages by up-regulating the activation of NF- κ B and MAPKs signaling pathway, and elevated the expression of MHC-II, CD40, CD80, and CD86. Upon stimulation with BC01, the peritoneal macrophages isolated from TLR9^{-/-} mice produced significantly low levels of pro-inflammatory cytokines, attenuated the activation of NF- κ B and MAPKs signaling pathways, and showed reduced phagocytosis. Following *in vivo* stimulation with BC01, the TLR9^{-/-} mice produced significantly lower levels of pro-inflammatory cytokines in the serum and lymph nodes showed reduced cell proliferation. These results indicate that BC01 is an efficient agonist of TLR9 that can significantly enhance the host-protective immune functions of macrophages.

Keywords

Adjuvant, innate immunity, macrophage, MAPKs pathway, NF- κ B pathway, TLR9

Date Received: 24 May 2019; revised: 5 September 2019; accepted: 8 September 2019

Introduction

Adjuvants are immune modulators that have been used for many decades in the treatment of various clinical manifestations. The incorporation of adjuvants into vaccine formulations is aimed at enhancing, accelerating, and prolonging antigen-specific immune responses. However, most of the vaccine adjuvants available for human or animal use were developed empirically, without a clear understanding of their cellular and molecular mechanism of action. Studies have shown that most of these adjuvants enhance the host T- and B-cell responses by engaging the components of the innate immune system, rather than directly affecting the respective lymphocytes themselves.^{1–4}

TLRs have been well demonstrated to play a critical role in the induction of innate and inflammatory

¹Division of Tuberculosis Vaccines, National Institutes for Food and Drug Control (NIFDC), Beijing, P.R. China

²NHC Key Laboratory of Human Disease Comparative Medicine, Institute of Laboratory Animal Sciences, Chinese Academy of Medical Sciences (CAMS) and Peking Union Medical College (PUMC), Beijing, P.R. China

³Beijing Key Laboratory for Animal Models of Emerging and Reemerging Infectious, Beijing, P.R. China

⁴Key Laboratory of Human Diseases Animal Model, State Administration of Traditional Chinese Medicine, Beijing, P.R. China

⁵Tuberculosis Center, Chinese Academy of Medical Sciences (CAMS), Beijing, P.R. China

⁶Public Health Research Institute (PHRI) center at New Jersey Medical School, Rutgers, The State University of New Jersey, Newark, USA

Corresponding author:

Aihua Zhao, NIFDC, No.31, Huatuo Rd., Biomedical Industry Park, Daxing District, Beijing, 102629, P.R. China.
Email: zhaoaihua2016@126.com



responses during infectious and non-infectious conditions.^{5–11} TLRs on APCs, such as macrophages and dendritic cells, can recognize incorporation of PAMPs expressed on a wide array of microbes, as well as endogenous danger-associated molecular patterns (DAMPs) released from dying cells; both PAMP and DAMP are capable of activating the host innate immune responses.^{12–14} Therefore, there has been an increasing focus on TLR research to develop and use the natural ligands or synthetic agonists as an adjuvant for immune stimulation, and several of these potential TLR adjuvants are in clinical or late pre-clinical stages at present.^{15,16}

TLR9 is thought to be able to activate the innate immune cells by detecting the unmethylated CpG dinucleotides, which are common in the genomes of most of the bacteria and DNA viruses. These CpG motif-containing regions are highly methylated in the vertebrate genomes.^{17–21} BC01, used in this study, was derived from unmethylated CpG motif-containing DNA fragment from the genome of BCG (BCG CpG DNA Combination adjuvants system 01). It has the following characteristics: (1) unmethylated CpG motifs: 15.75%–24.75%; (2) relative MW range: 3000–10,000 base pairs; (3) natural bases and more stable; and (4) no species differences. However, it has been well documented that synthetic oligonucleotides, such as CpG-oligo-deoxynucleotides (CpG-ODNs), contain unmethylated CpG dinucleotides, in particular sequence contexts (CpG motifs). These CpG motifs are present at a 20-fold higher frequency in bacterial DNA compared with mammalian DNA. Their relative MW range is 20–30 bases, such as ODN 2395 (5'-tcgt cgttttcggcgcgcgccg-3', 22mer); although these synthesized CpG are phosphorothioate-modified to improve their function and bioavailability, they are easily degradable and show species differences simultaneously. Nonetheless, ODNs containing unmethylated CpG motifs can act as immune adjuvants to up-regulate and activate Th1 response, associated with production of pro-inflammatory cytokines, and support the maturation of APCs in humans and animal models.^{22–25}

Successful engagement of TLR ligands with cognate receptors triggers a signal transduction cascade that results in the activation of NF- κ B and MAPKs pathways,²⁶ which induce a pro-inflammatory response. Upon engagement with a ligand, all TLRs, except for TLR3, recruit the adaptor protein MyD88 to the TIR domain on IRAK-4, resulting in phosphorylation of IRAK-1, which through a series of steps involving TRAF-6, leads to the activation of NF- κ B.^{27,28} Translocation of NF- κ B from the cytoplasm into the nucleus regulates the expression of genes involved in various cellular processes, such as cell survival, proliferation, and the regulation of pro-inflammatory cytokines.²⁹ In addition, depending on the type and nature,

TLR signaling can also activate MAPKs, including p38 kinase, c-Jun-N-terminal kinase (SPAK/JNK) and extracellular-regulated kinase (Erk1/2),^{13,28,30,31} all of which are capable of activating pro-inflammatory cascades, either directly or indirectly through various transcription networks in host immune cells.^{32–34}

The adjuvant reported in this study, BC01, exhibits strong adjuvant properties and without species differences in eliciting significantly improved immunogenicity when combined with a recombinant/sub-unit protein, polysaccharide, or inactivated vaccines derived from bacteria, viruses, and parasites.^{35–38} Though the ability of BC01 as an adjuvant component to recombinant tuberculosis vaccine is being tested in clinical trials, the mechanisms and signaling pathway underlying the host immune activation by BC01 remain unclear. Therefore, the main objective of this study was to identify and explore the molecular signaling mechanism of BC01 in the activation of macrophages, which are primary APCs of the innate host immunity. We wanted to test the effect of BC01 on macrophage responses, explicitly mediated by the NF- κ B and MAPK pathways since these are major regulatory factors involved in host inflammation and innate immunity.

Materials and methods

Mice and cell line

Specific Pathogen-Free (SPF) C57BL/6 mice and TLR9^{-/-} mice were purchased from the Institute for Laboratory Animal Resources, National Institutes for Food and Drug Control, Beijing, China (C57BL/6 and TLR9^{-/-} mice: Female, 8 wk old, 18–22 g). Mice were housed in the experimental animal center at NIFDC and fed commercial mouse chow and water *ad libitum*. All the experimental procedures were in accordance with the institutional guidelines for the ethical handling of animals and were approved by the institutional ethical committee. The mouse macrophage cell line (RAW 264.7) was purchased from Procell Life Science & Technology Co. Ltd, Wuhan, China and cultured in DMEM, supplemented with 10% FBS, 100 U/ml penicillin and 100 μ g/ml streptomycin and maintained at 37°C in a humidified incubator with 5% CO₂ supply.

Preparation of BC01

BC01 was derived from genomic DNA fragments of *Mycobacterium bovis* BCG. Briefly, the bacteria were grown for 14–20 d in Sauton's broth, pelleted, washed and suspended at 200 mg/ml concentration in deionized, sterile distilled water. The cells were homogenized with a

tissue homogenizer as three pulses of 3 min each, and the homogenate was subjected to high-speed freeze ultra-centrifugation, and the supernatant was collected. The double-stranded DNA fragments extracted from BCG were purified by Q Sepharose HP ion-exchange chromatography, and the purified BC01 was concentrated by ultrafiltration and stored at -20°C . Biochemical analysis of BC01 for quality and constituents in breakthrough peak and eluted peaks was done with Lowry method (protein), Anthrone measurement (polysaccharides) and 0.8% agarose gel electrophoresis (RNA). For some experiments, 1 mg/ml of BC01 was incubated with 1 KU DNase I at 37°C for 12 h and inactivated for 10 min at 65°C . The quality and quantity of purified DNA, with or without DNase treatment, was evaluated using 0.7% agarose gel electrophoresis.

Isolation of mouse peritoneal macrophages

TLR9^{-/-} or C57BL/6 mice were injected intraperitoneally with 2 ml of 4% thioglycolate 3 d before sacrifice, and the peritoneal cavities were flushed with 8 ml of RPMI 1640 medium. Cells from the peritoneal wash were collected by centrifugation and washed in fresh media. After washing, 5×10^5 cells/well were plated in 24-well cell culture plates with RPMI 1640 media and incubated for 4 h at 37°C with 5% CO₂ supply. Non-adherent cells were removed from the plates by washing twice with DMEM media, and the small peritoneal macrophages were treated with 7.5 μg/ml of BC01, or other stimulants (see below) in DMEM media containing 10% FBS, 100 U/ml penicillin, and 100 μg/ml streptomycin at 37°C with 5% CO₂ supply.

Cytokine ELISA

Cytokine ELISA MAXTM Deluxe Kit (BioLegend, USA) was used to measure the cytokine levels, and the experiments were performed as per the manufacturer's instructions. The following inhibitors were used to block various signaling molecules in RAW 264.7 cells: 2 μM of an antagonist-inhibitory ODN 2088 (for TLR9), 10 μM of JSH-23 (for NF-κB), 1 μM of SB203580 (for p38 kinase), 10 μM of SP600125 (for SPAK/JNK kinase), 5 μM of PD98059 (for Erk1/2 kinase). In these inhibitor assays, 5×10^5 cells/well RAW 264.7 cells were pre-treated for 12 h at 37°C with respective chemical blocker followed by stimulation of the cells with 7.5 μg/ml BC01 and ODN 2395 (Invivogen, USA). In another experiment RAW 264.7 cells were pre-treated for 0.4 h at 37°C with 7.5 μg/ml BC01 followed by incubation with the same concentration of chemical blocker for 24 h. Cell culture supernatants were collected after 24 h incubation with BC01 or ODN 2395 and TNF-α, and MCP-1 levels were measured using ELISA. All the inhibitors,

except ODN 2088 were purchased from Sigma-Aldrich Co. LLC., St. Louis, USA; ODN 2088 was obtained from Invivogen, USA, and used as recommended by the manufacturers. Each experiment was repeated at least three times independently.

Total RNA isolation

RAW246.7 cells were stimulated for various time points (0.5 to 48 h) with different concentrations (0, 0.75, 1.5, 7.5, 15 or 75 μg/ml) of BC01 either pre-treated (7.5 μg/ml) with DNase I or without any treatment. After stimulation, the cells were washed twice with PBS and 1 ml of *TransZol* UP (TransGen Biotech Company, China) was added to each well and vigorously mixed to lyse the cells. The lysate was mixed with 200 μl chloroform, incubated for 3 min at 25°C and centrifuged to separate the aqueous phase from the organic phase. Isopropanol was added to the aqueous phase (1:1), and samples were incubated at -20°C for 2 h and centrifuged to precipitate the total RNA. The precipitate was washed twice with 1 ml of ice-cold 75% ethanol, air-dried and dissolved in RNase-free water. The quantity and quality of isolated total RNA were checked using agarose gel electrophoresis.

RT-PCR and qRT-PCR analysis

The total RNA was used for first-strand cDNA synthesis via reverse transcription using *TransScript* One-Step gDNA Removal and cDNA Synthesis SuperMix kit (TransGen Biotech Company, China). Reverse transcription-PCR (RT-PCR) was carried out using *TransTap* High Fidelity PCR SuperMix I Kit (TransGen Biotech Company, China) in an Applied Biosystems PCR system 2400 (Thermo Fisher Scientific, USA). The amplified target gene product was visualized using 1.0% agarose gel electrophoresis with a Vilber Infinity 3026 (Vilber Lourmat, France). Quantitative real-time PCR (qRT-PCR) reactions were carried out in a CFX96 Real-Time PCR Detection System (Biorad, USA). Each 20 μl reaction mixture was comprised of 10 μl of ChamQ SYBR qPCR Master Mix (Vazyme, China), 7.5 μl of deionized water, 2 μl of 10-fold diluted template, and 0.5 μl of each amplification primer. The cycling conditions were set as follows: initial denaturation of 95°C for 30 s, followed by 40 cycles of denaturation at 95°C for 5 s, annealing at 60°C for 30 s. The melting curves were then performed by heating the amplicon from 65 to 95°C . Negative controls without template were also included at the same time to ensure amplification quality. Transcript levels of reference genes were performed in three independent biological samples, each with three technical replicates. The amplification efficiency

(E , $E = 10^{[-1/\text{slope}] - 1}$) and the correlation coefficients (R^2) for each primer were calculated by utilizing standard curves with ten-fold serial dilutions. The β -actin was used as the internal standard. All gene-specific primers were synthesized by Sangon (Shanghai, China), and their sequences (5'-3') are as follows: β -actin (TGTTACCAACTGGGACGACA and CTGGGTCATCTTTTCACGGT), TNF- α (CCCACGTCGTAGCAAACCA and GGCAGAGAGGAGGTTGACTT), MCP-1 (TCTGTGCTGACCCCAAGAAG and AGGCATCACAGTCCGAGTCA).

Analysis of subcellular NF- κ B localization

RAW 264.7 cells were seeded into 8-well culture plates with glass coverslips and were treated either directly with 7.5 μ g/ml BC01 for 0, 15, 30, 60, 120, 180, and 240 min or after 12 h pre-treatment with the inhibitors ODN 2088 and JSH-23. Cells were washed thrice with sterile PBS, fixed with 4% paraformaldehyde for 15 min, permeabilized in sterile PBS, containing 5% Triton X-100 for 20 min, and were washed with PBS. To avoid non-specific binding of Abs, the cells were primarily incubated with 5% blocking serum for 30 min before the incubation with rabbit anti-mouse NF- κ B Ab (Santa Cruz, USA). After 12 h incubation, the cells were washed, FITC-conjugated goat anti-rabbit IgG (Santa Cruz, USA) was added, and the cells were incubated for an additional 1 h at 37°C. After washing with PBS, the cells were incubated with 500 ng/ml DAPI for 5 min at 25°C. The coverslips with cells were observed and photographed using Ultra VIEW Vox-3D Live Cell Imaging System (PerkinElmer, Inc, UK) at $\times 100$, oil immersion objective, and each experiment was repeated at least three times independently.

Phospho-specific protein microarray analysis

Phosphoprotein detection assays were performed in cooperation with Wayen Biotechnology, Shanghai, China. Briefly, 100 μ g lysate of RAW 264.7 cells treated for 45 min with 7.5 μ g/ml BC01 or ODN 2395 was labeled with biotin and hybridized with the NF- κ B Pathway Phosphorylation Antibody Array Kit (Full Moon Biosystems Inc, USA). This ELISA-based microarray is suitable for protein phosphorylation profiling. The slides were scanned with a Gene Pix 4000B scanner, and the fluorescence intensity was measured using Gene Pix Pro 6.0 software. The raw data were analyzed using Grubbs' method and the phosphorylation ratio was computed as follows: Phospho Ratio = (phosphorylated_(Exp.)/unphosphorylated_(Exp.))/(phosphorylated_(Con.)/unphosphorylated_(Con.)) where Exp. represents the test samples and Con. represents the control. Each of the Abs has six replicates that are

printed on a coated glass microscope slide, along with multiple empty or positive markers and negative controls.

Image Stream analysis

For the Image Stream analysis, 5×10^5 cells/well of RAW 264.7 cells were pre-treated with or without the inhibitors of p38, SPAK/JNK or Erk1/2 for 12 h followed by stimulation with BC01 for 45 min at 37°C. The cells were incubated 12 h at 4°C with 100 μ l primary Ab diluted 1:200 in permeabilization buffer. The cells were fixed with 4% paraformaldehyde for 15 min at 25°C. After washing with PBS, the cells were incubated with 100 μ l FITC-conjugated mouse anti-rabbit IgG (Santa Cruz, USA) for 1 h at 37°C. The cells were washed, suspended in 200 μ l of 500 ng/ml DAPI for 5 min at 25°C, and the fluorescent images were visualized using Amnis Image Stream 100 (EMD Millipore Corp, Darmstadt, Germany).

In vitro phagocytosis assay

The phagocytosis assay was performed according to the following two methods: (1) for Image Stream (Amnis) analysis, 5×10^5 cells/well of RAW 264.7 cells were stimulated for 24 h with BC01 and were incubated with 1×10^6 FluoroSpheresTM Carboxylate-Modified Microspheres for 2 h. After incubation, the cells were washed with PBS and were labeled with APC-F4/80 Ab at 37°C for 30 min and examined under Amnis Image Stream Data Analyzer, equipped with the Amnis INSPIRE software. The percentages of cells for internalization was analyzed using the Amnis IDEAS software (EMD Millipore Corp, Darmstadt, Germany); (2) for laser scanning confocal microscopy, 5×10^5 cells/well of peritoneal macrophages from C57BL/6 or TLR9^{-/-} mice were seeded into the 8-well culture plates. After 24 h pre-treatment with 7.5 μ g/ml BC01, the cells were incubated with 1×10^6 FluoroSpheresTM Carboxylate-Modified Microspheres for 2 h. Then, the cells were labeled with APC-conjugated anti-mouse F4/80 Ab at 37°C for 30 min. Finally, the cells were blocked with an anti-fluorescence quenching agent and observed using Ultra VIEW Vox-3D Live Cell Imaging System (PerkinElmer, Inc, UK) at $\times 100$, oil immersion objective, and each experiment was repeated at least three times independently.

Protein preparation and Western blot analysis

RAW 264.7 cells and mouse peritoneal macrophages (5×10^5 cells/condition/time point) were stimulated for various time points (0, 15, 30, 45, 60, and 120 min) and then treated with the cell lysis buffer supplemented with 1 μ g/ml aprotinin (Amresco, USA). The

cell lysates were centrifuged at 12,000 *g* for 30 min at 4°C, and the protein concentration in the supernatant was measured using the BCA protein assay (Solarbio, China). Equal amounts (10 µg) of protein were separated by SDS-PAGE and transferred to polyvinylidene fluoride membranes. After blocking with 5% goat blocking serum, the membranes were incubated 12 h at 4°C with primary Abs, including p38 MAPK Ab, phospho-p38 MAPK Ab, SAPK/JNK Ab, Phospho-SAPK/JNK Ab, p44/42 MAPK (Erk1/2) Ab and phospho-p44/42 MAPK (Erk1/2) Ab, according to the manufacturer's instructions (Cell Signaling Technology, USA). After washing with TBST buffer, the membranes were incubated with the appropriate HRP-conjugated mouse anti-rabbit IgG secondary antibodies for 1 h at 37°C. Finally, the membranes were treated with Pro-light HRP Chemiluminescent solution (Millipore, Germany), and the chemical luminescence was measured.

Flow cytometric analysis

RAW 264.7 cells and mouse peritoneal macrophages (5×10^5 cells/well) were incubated in 24-well plates with 7.5 µg/ml BC01 for 12, 24, or 48 h. The cells were harvested and washed with sterile PBS and were incubated with FITC-conjugated anti-mouse CD40 (Clone: HM40-3, Biolegend, USA), APC-conjugated anti-mouse CD80 (Clone: 16-10A1, Biolegend, USA), PE-conjugated anti-mouse CD86 (Clone: GL-1, Biolegend, USA), and Percp/Cy5.5-conjugated anti-mouse I-A/I-E (Clone: M5/114.15.2, BioLegend, USA) for 30 min in the dark. Finally, the cells were fixed with 1% paraformaldehyde and were analyzed using a FACScan flow cytometer. In the experiments designed to block TLR9, the RAW 264.7 cells were pre-treated with a specific 2 µM ODN 2088 inhibitor for 12 h at 37°C.

In vivo stimulation of mice and isolation of APCs

Wild type and TLR9^{-/-} ($n = 10$ per strain) female mice ($n = 10$) were injected with BC01 at 0, 3, and 7 d. Mice in the test group underwent intramuscular (i.m.) injection of 100 µl of sterile PBS containing 750 µg/ml of BC01. Mice in the negative control group were injected i.m. with 100 µl of sterile PBS. The mice were euthanized by cervical dislocation 3 d after the final injection. APCs from the inguinal lymph node were isolated and analyzed using the flow cytometry. The serum was separated from the whole blood to measure the levels of inflammatory cytokines.

Statistical analysis

Results are reported as the mean ± S.D. ($n = 3$). Analytical testing was conducted by one-way ANOVA, followed by Tukey test, using Statistical Program for Social Sciences 19.0 (SPSS Inc., Chicago, USA). For all analyses, $P < 0.05$ was considered statistically significant.

Results

Characterization of BC01

The BC01 used in this study is a double-stranded DNA fragment of BCG with a size between 3 and 10 kbp. The DNA fragments were extracted from the BCG vaccine by Q Sepharose HP ion-exchange chromatography (Figure S2). To demonstrate that these DNA fragments contain unmethylated CpG motif, first, we treated the BC01 with CpG methyltransferase (M.SssI), an enzyme that methylates all cytosine residues in a double-stranded DNA fragment. This was followed by restriction digestion of M.SssI-treated BC01 with HpaII (a specific restriction endonuclease that recognizes the sequence 5'-CCGG-3'). The rationale for this step is that nucleotides in the DNA that have been methylated by M.SssI will not be cleaved/restricted by HpaII. As shown in Supplemental Figure 1 treatment with HpaII cleaved the native BC01 (lanes 3 and 7) from the size between 3–10 kbp to 100–250 bp (lanes 4 and 8). However, in BC01 methylated with M.SssI, the larger DNA fragment (3–10 kbp) remains intact and not cleaved by HpaII (lanes 2 and 6). We also show that M.SssI treatment did not shear the 3–10 kb DNA fragments (lanes 1 and 5). Based on these observations, we believe that BC01 contains a large amount of unmethylated CpG motif-containing DNA of BCG. The purity values of BC01 as determined by spectrophotometer are $A_{260}/_{280} = 1.8$ and $A_{260}/_{230} = 2.2$. The detailed biochemical analysis of BC01 is shown in Figure S2 and Table S1.

BC01 stimulation triggers the production of pro-inflammatory cytokines by murine macrophages

To determine the effect of BC01 on the activation of macrophages, the number of pro-inflammatory markers, TNF-α and MCP-1, at the protein and gene transcription levels, was measured using ELISA or qRT-PCR assays. As shown in Figure 1, BC01 stimulation significantly enhanced the production of TNF-α and MCP-1 at both the protein ($P < 0.001$ and $P < 0.001$, Figure 1(a)) and gene expression ($P < 0.001$ and $P < 0.001$, Figure 1(b)) levels, in a dose-dependent

manner up to 7.5 $\mu\text{g/ml}$ (Figures S3a and S3c). The protein and transcript of these two cytokines were detected at 3 h post-stimulation with BC01 and peak levels were noted at 24 h ($P < 0.01$, $P < 0.01$, Figure S3b, and $P < 0.01$, $P < 0.01$, Figure S3d). To confirm that the observed results are due to the stimulation by CpG DNA present in BC01 and not due to

any contaminating components, BC01 (7.5 $\mu\text{g/ml}$) was treated with DNase I and the experiment were repeated. The results show that DNase I treatment significantly abrogated the BC01-induced production of TNF- α and MCP-1 at the protein and gene transcription levels (all $P > 0.05$, lane 2 in Figure 1(a), (b), and (c)), compared with no treatment control, confirming

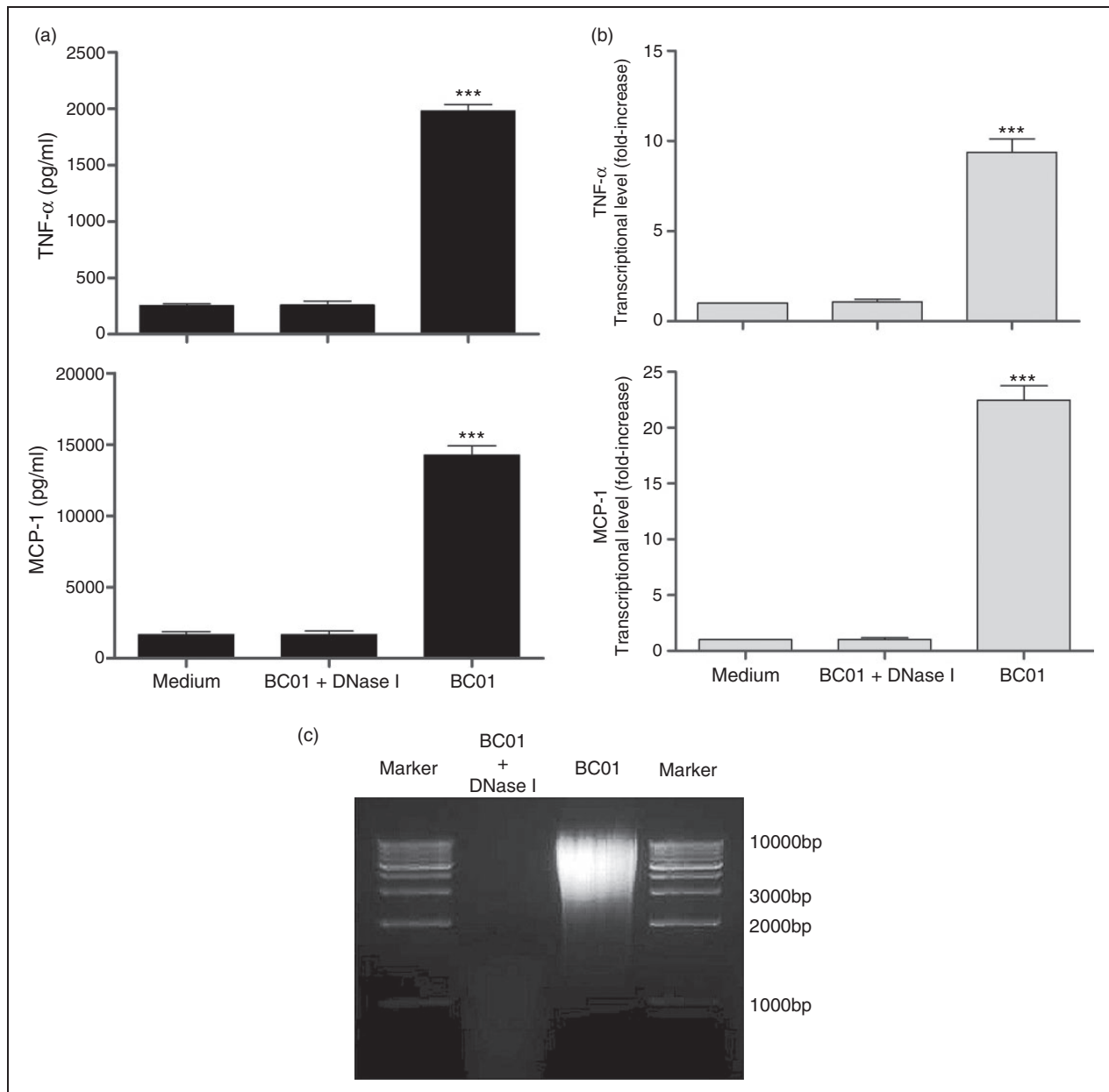


Figure 1. BC01 stimulation induces secretion of cytokines by murine macrophages. RAW 264.7 cells were stimulated with BC01 for 24 h at 7.5 $\mu\text{g/ml}$ of BC01 with or without DNase I pre-treatment. (a) Culture supernatants were collected, and the amount of TNF- α and MCP-1 levels were measured using ELISA. (b) qRT-PCR estimation of TNF- α and MCP-1 mRNA levels in RAW 264.7 cells. (c) Image of agarose gel electrophoresis of BC01 with (lane 2) or without (lane 3) DNase I pre-treatment. Data in (a) and (b) are expressed as mean \pm SD from at least three independent experiments, *** $P < 0.001$. Data in (c) are representative images of three independent experiments.

that the nucleic acid component in BC01 was responsible for the induced production of TNF- α and MCP-1.

BC01 stimulation promotes translocation of NF- κ B subunits to the nucleus

NF- κ B, one of the crucial transcription factors activated during TLR signaling, works as a dimer formed by the interactions of two of the five Rel family proteins. In resting cells, NF- κ B is restricted in the cytoplasm by its binding with the inhibitory factor I κ B α . Activation of the TLR signaling pathway degrades I κ B α and releases the NF- κ B, and the phosphorylated NF- κ B translocates to the nucleus to function as a transcription factor. In this study, the effect of BC01 on the translocation and activation of NF- κ B was examined using confocal laser scanning microscope and phosphoprotein microarray. The confocal microscopic images revealed the localization of NF- κ B p65 to the nucleus in the BC01-treated cells. Compared with the untreated cells, active translocation of NF- κ B p65 into the nuclei was noticed at 15 min after the BC01 stimulation that reached a maximum at 60 min; however, the level was decreased after 120 min of stimulation (Figure 2(a)). Next, we tested the extent of phosphorylation of molecules in the NF- κ B pathway between BC01-treated and ODN 2395-treated cells. Consistent with the confocal laser scanning microscope findings, RAW 264.7 cells stimulated with 7.5 μ g/ml BC01 had significantly increased phosphorylation of molecules in NF- κ B signaling, including NF- κ B p65, NF- κ B p105/p50, and NF- κ B p100/p52 (Figure 3(a)), compared with the unstimulated controls. Among the up-regulated phosphorylation signal molecules, expression of six was generally increased in both BC01 and ODN 2395-stimulated

cells (Figure 3(b)); however, the phosphorylation signals were decreased for four of the 13 molecules (Figure 3(c)).

Activation of NF- κ B signaling pathway underlies BC01-mediated macrophage activation

The NF- κ B signaling pathway is one of the key processes in the innate immune responses, and NF- κ B is a pivotal transcription factor that plays an important role in the production of pro-inflammatory cytokines. To determine whether BC01 stimulation of macrophage activation is achieved by the NF- κ B signaling pathway, we treated RAW 264.7 cells with a specific NF- κ B inhibitor, JSH-23, before its stimulation with BC01. The results showed that the nuclear translocation of NF- κ B was blocked by JSH-23 (Figure 4(c)), which leads to a significantly attenuated production of TNF- α and MCP-1 (Figures 4(a), $P < 0.01$, and 4(b), $P < 0.01$). Consistent with these results, JSH-23 treatment of RAW 264.7 cells after BC01 stimulation significantly reduced the levels of TNF- α and MCP-1 (Figures 4(d), $P < 0.001$, and 4(e), $P < 0.001$).

TLR9 mediates NF- κ B nuclear translocation and cytokine production in BC01-stimulated macrophages

After establishing the effect of BC01 in promoting NF- κ B activation and its nuclear translocation, we determined whether TLR9 is involved in these processes. Hence, macrophages were treated with a TLR9 antagonist, ODN 2088, which significantly attenuated the nuclear translocation of NF- κ B (Figure 5(c)). Consequently, the production of TNF- α and MCP-1 was significantly reduced upon pre-treatment of

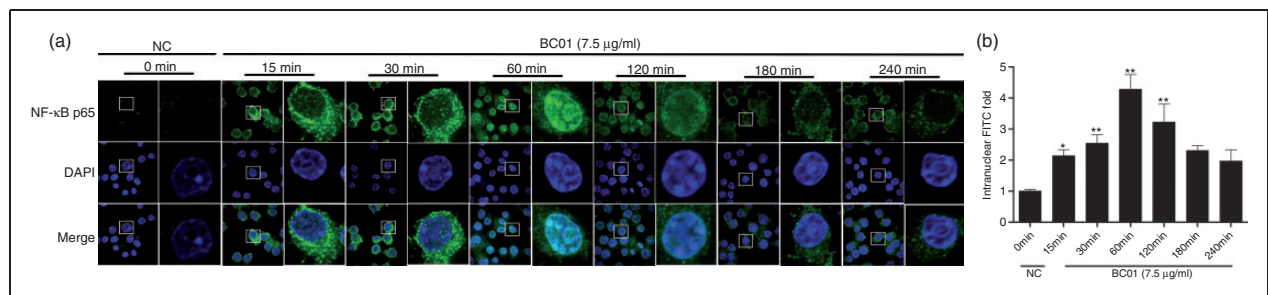


Figure 2. BC01 stimulation promotes nuclear translocation of NF- κ B in murine macrophages. Confocal microscopy (original magnification $\times 100$, oil immersion objective) was used to determine the effect of BC01 stimulation on the translocation of NF- κ B from the cytoplasm to the nucleus in RAW 264.7 cells. (a) RAW 264.7 cells in growth medium alone (0 min) or 7.5 μ g/ml BC01 for the pre-determined time points (15–240 min). (b) The histogram represents relative nuclear FITC fluorescence intensity at various time points. Data in (b) are expressed as mean \pm SD from at least three independent experiments. NC denotes negative control; * $P < 0.05$, ** $P < 0.01$.

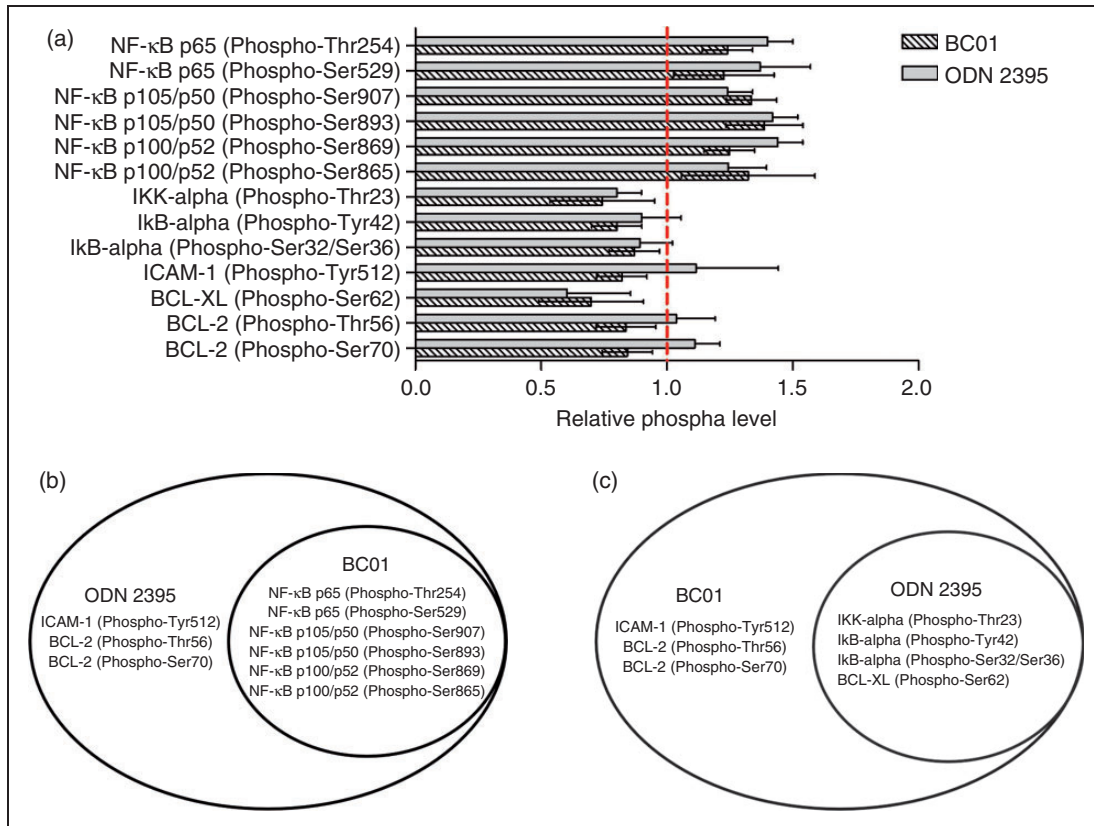


Figure 3. Phosphoprotein analysis of NF-κB signaling pathway in BC01-stimulated murine macrophages. (a) Phosphorylated signal proteins in RAW 264.7 cells that were either unstimulated or stimulated with 7.5 μg/ml BC01 or ODN 2395 were measured using an Ab microarray system and comprehensively analyzed. The phosphorylation ratio was computed as follows: $\text{PhosphoRatio} = (\text{phosphorylated(Exp.)}/\text{unphosphorylated(Exp.)})/(\text{phosphorylated(Con.)}/\text{unphosphorylated(Con.)})$, where Con. denotes no stimulation and Exp. denotes BC01 or ODN 2395 stimulation. Relative phosphate level > 1 means increased phosphorylation, and a relative phosphate level < 1 means decreased phosphorylation. (b) The phosphorylation signal molecules that were induced in the BC01 or ODN 2395-stimulated samples. (c) The phosphorylation signal molecules that were dampened in the BC01 or ODN 2395-stimulated samples.

macrophages with ODN 2088 for 12h followed by stimulation with BC01 or ODN 2395, a known stimulant of TLR9 (Figures 5(a), $P < 0.01$ and 5(b), $P < 0.01$). Furthermore, we used C57BL/6 and TLR9^{-/-} mice to analyze whether TLR9 mediated the production of these pro-inflammatory cytokines upon stimulation by BC01. Peritoneal macrophages isolated from C57BL/6 and TLR9^{-/-} mice and were stimulated with BC01 or ODN 2395. We observed a significantly lower production of TNF-α and MCP-1 in the macrophages of TLR9^{-/-}, compared with the C57BL/6 mice, after BC01 stimulation (Figures 5(d), $P < 0.01$ and 5(e), $P < 0.01$). In these cells, the results obtained with the ODN 2395 stimulation were similar to those observed with BC01 stimulation. These results indicate that the effects of BC01 on macrophage function, including NF-κB activation and its nuclear translocation as well as induction of TNF-α and MCP-1 secretion, involve TLR9 signaling.

BC01 stimulation promotes phosphorylation of p38, SPAK/JNK, and Erk1/2

To determine whether BC01 activates the MAPK pathway, we performed Western blot analysis on macrophages after stimulation with BC01. The phosphorylation status of MAPKs pathways was detected in the Western blot analysis. Treatment of RAW 264.7 cells with BC01 induced a robust phosphorylation of p38, SPAK/JNK, and Erk1/2 after 15–45 min; peak phosphorylation of p38, SPAK/JNK, and Erk1/2 occurred within 45, 30, and 15 min of stimulation, respectively, and then returned to baseline at/after 60 min of stimulation with BC01 (Figure 6).

BC01-induced cytokine expression involves activation of the MAPK signaling pathway

To investigate the role of MAPK in BC01-mediated activation of the innate immune response,

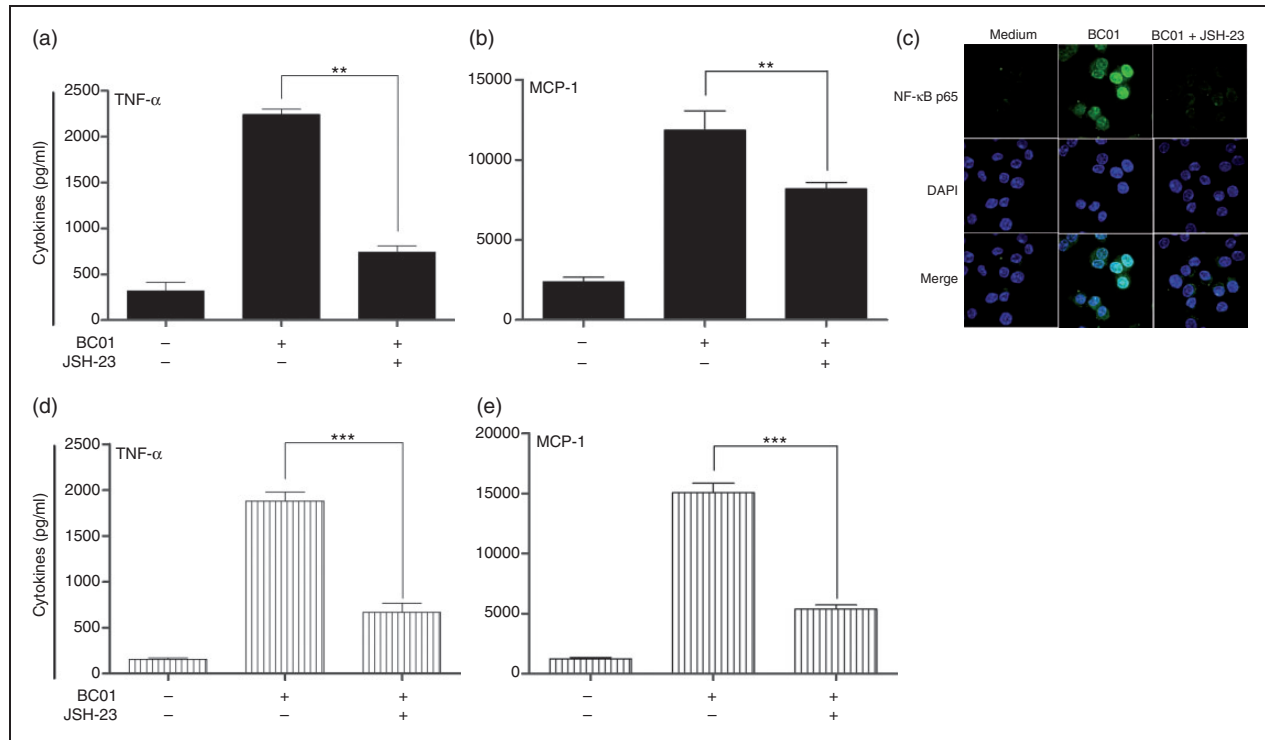


Figure 4. Effect of NF- κ B inhibition on cytokine production by BC01 stimulated murine macrophages. (a) and (b) RAW 264.7 cells were treated with or without NF- κ B specific inhibitor JSH-23 for 12 h followed by incubation with complete medium alone or with 7.5 μ g/ml of BC01 for 24 h. Concentrations of TNF- α and MCP-1 in the cell culture supernatant were measured using ELISA. (c) Confocal microscopy (original magnification $\times 100$, oil immersion objective) was used to determine the nuclear translocation of NF- κ B after incubation with medium alone or with BC01 for 1 h. (d) and (e) RAW 264.7 cells were treated with 7.5 μ g/ml of BC01 for 0.4 h, followed by incubation with or without NF- κ B specific inhibitor JSH-23 for 24 h. Concentrations of TNF- α and MCP-1 in the cell culture supernatant were measured using ELISA. Data shown are mean \pm SD from at least three independent experiments. ** $p < 0.01$, *** $p < 0.001$.

macrophages were treated with p38 (SB203580, 1 μ M), SPAK/JNK (SP600125, 10 μ M), or Erk1/2 (PD98059, 5 μ M) inhibitors, before and after BC01 stimulation, and the production of TNF- α and MCP-1 was measured (Figure 7). While BC01 treatment alone induced the expression of TNF- α and MCP-1, pre-treatment of macrophages with SP600125 significantly reduced the levels of these cytokines (Figures 7(a), $P < 0.01$, and 7(b), $P < 0.001$). The expression of TNF- α , and not MCP-1, was partially inhibited by PD98059 (Figure 7(a), $P < 0.01$). However, pre-treatment of cells with SB203580 did not show significant inhibition on the expression of these cytokines by the treated macrophages. These results were also confirmed by independent experiments in which RAW 264.7 cells were stimulated with BC01 for 0.4 h followed by treatment with the inhibitors at same concentration as described above (Figures 7(c), $P < 0.05$, $P < 0.001$, $P < 0.01$, and 7(d), $P < 0.001$, $P < 0.01$). The cytokine ELISA data are consistent and confirmed by protein analysis using Western blot, which showed that SB203580, SP600125, or PD98059 inhibited the activity

of respective kinases and abolished BC01-induced phosphorylation of p38, SPAK/JNK, and Erk1/2, respectively (Figure 8(a)). To quantitatively analyze the degree of p38, SPAK/JNK, and Erk1/2 phosphorylation followed by BC01 treatment, we collected the fluorescent cell images using the Image Stream 100. Consistent with the Western blot analysis, the percentages of phosphorylated SPAK/JNK and Erk1/2 in the nucleus peaked at 31.3% and 40.3% after 30 min of stimulation with BC01 (Figures 7(f) and 7(g)). However, the SPAK/JNK and Erk1/2 phosphorylation was significantly decreased to 4.65% and 18.1% in the cells which were pre-treated with the inhibitors, compared with the untreated cells (Figures 7(f) and 7(g)). These results link a causal role for phosphorylation of MAPK signaling pathway in BC01-induced production of pro-inflammatory cytokine by macrophages.

BC01 activation of MAPK signaling pathway involves TLR9

To determine the role of TLR9 in the BC01-activated MAPK signaling pathway, we measured the

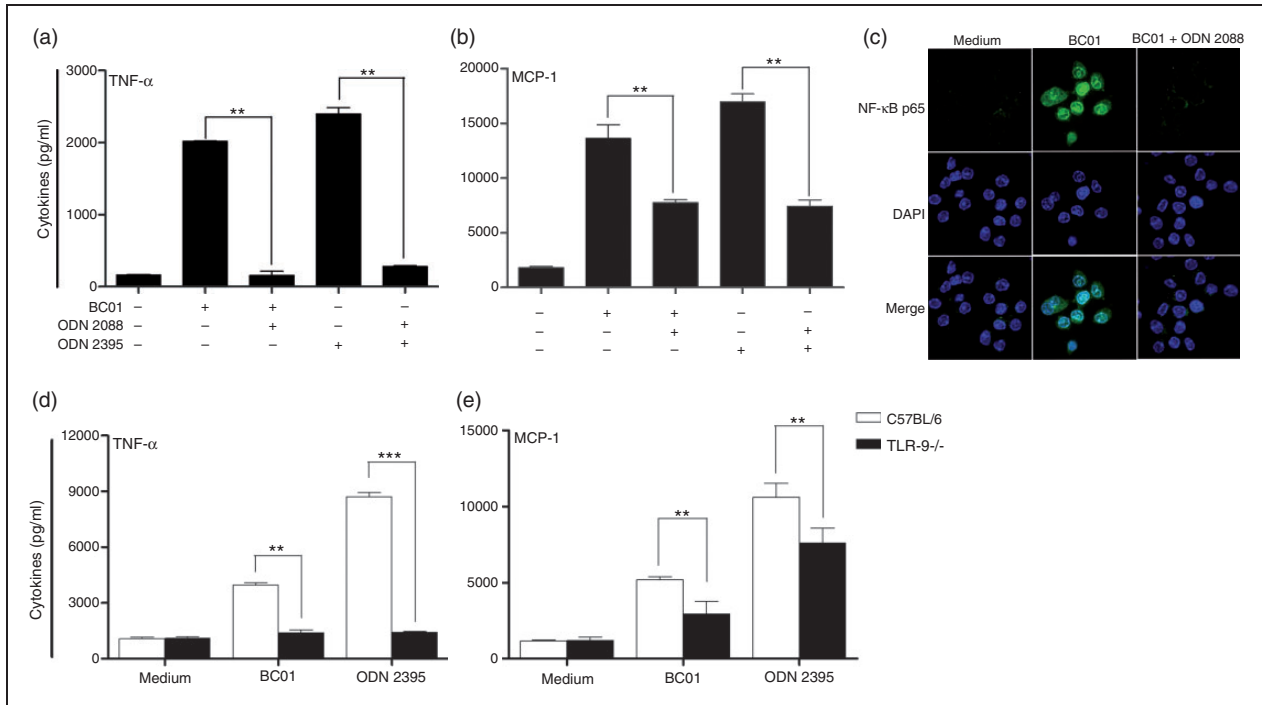


Figure 5. TLR9 mediates the NF- κ B nuclear translocation, and cytokine production in BC01-stimulated murine macrophages. (a) and (b) RAW 264.7 cells were treated with or without TLR9 antagonist, ODN 2088 for 12 h followed by stimulation with 7.5 μ g/ml of BC01 or ODN 2395. After 24 h of incubation, culture supernatants were collected, and the amounts of TNF- α and MCP-1 were measured using ELISA. (c) RAW 264.7 cells were treated with or without TLR9 antagonist ODN 2088 for 12 h, followed by stimulation with 7.5 μ g/ml of BC01. After 1 h of stimulation, confocal microscopy (original magnification \times 100, oil immersion objective) was used to determine the nuclear translocation of NF- κ B p65. (d) and (e) Peritoneal macrophages from C57BL/6 or TLR9^{-/-} mice were treated with complete medium, 7.5 μ g/ml of BC01 or 7.5 μ g/ml of ODN 2395 for 24 h. The amounts of TNF- α and MCP-1 in the supernatants were measured using ELISA. Data are expressed as the mean \pm SD from three independent experiments. ** $P < 0.01$, *** $P < 0.001$.

phosphorylation levels of p38, SPAK/JNK, and Erk1/2 in the peritoneal macrophages isolated from C57BL/6 or TLR9^{-/-} mice by Western blot analysis. As shown in Figure 8, BC01-mediated phosphorylation of the above kinases was attenuated in the peritoneal macrophages of TLR9^{-/-} mice. Similarly, a minimal level of phosphorylation was observed in the macrophages obtained from wild type C57BL/6 mice upon pre-treatment with a TLR9 antagonist, ODN 2088. These results suggest that the activation of the MAPK signaling pathway is potentially mediated by TLR9 signaling.

BC01 enhances macrophage phagocytosis through TLR9

To determine the effect of BC01 on macrophage phagocytosis, Amnis cellular imaging technology was used. This method has been used to observe and visualize the interactions between the phagocytes and the target microspheres and is capable of quantitating phagocytes positive for internalized targets. We have adopted this technique to verify the role of TLR9 in BC01-mediated

phagocytosis by macrophages. A representative image of RAW 264.7 cells with engulfed FluoroSpheresTM Carboxylate-Modified microsphere is shown in Figure 9(a). Quantitative imaging analysis of phagocytosis using Amnis IDEAS software indicated that BC01 and ODN 2395 significantly enhanced macrophage phagocytosis (52.5% and 58.7%, respectively), compared with the untreated cells (27.7%; $P < 0.01$ and $P < 0.01$; Figure 9(b)). This TLR9-mediated phagocytosis was further confirmed by ODN 2088 treatment of macrophages, which significantly reduced the internalization of the fluorescent beads (52.3% versus 36.7%, $P < 0.01$; Figure 9(b)). In addition, we determined the percent phagocytosis from the number of macrophages that consumed at least one fluorescent microsphere to the total number of cells in the same visual field, using confocal microscopy (Figure 10). The results indicate that the phagocytic rate of the peritoneal macrophages isolated from C57BL/6 mice was significantly higher (mean: 63.2%; $P < 0.01$) than the TLR9^{-/-} mice (mean: 41.1%) (Figure 10(b)). Similarly, evaluation of the phagocytic index of individual macrophages in the

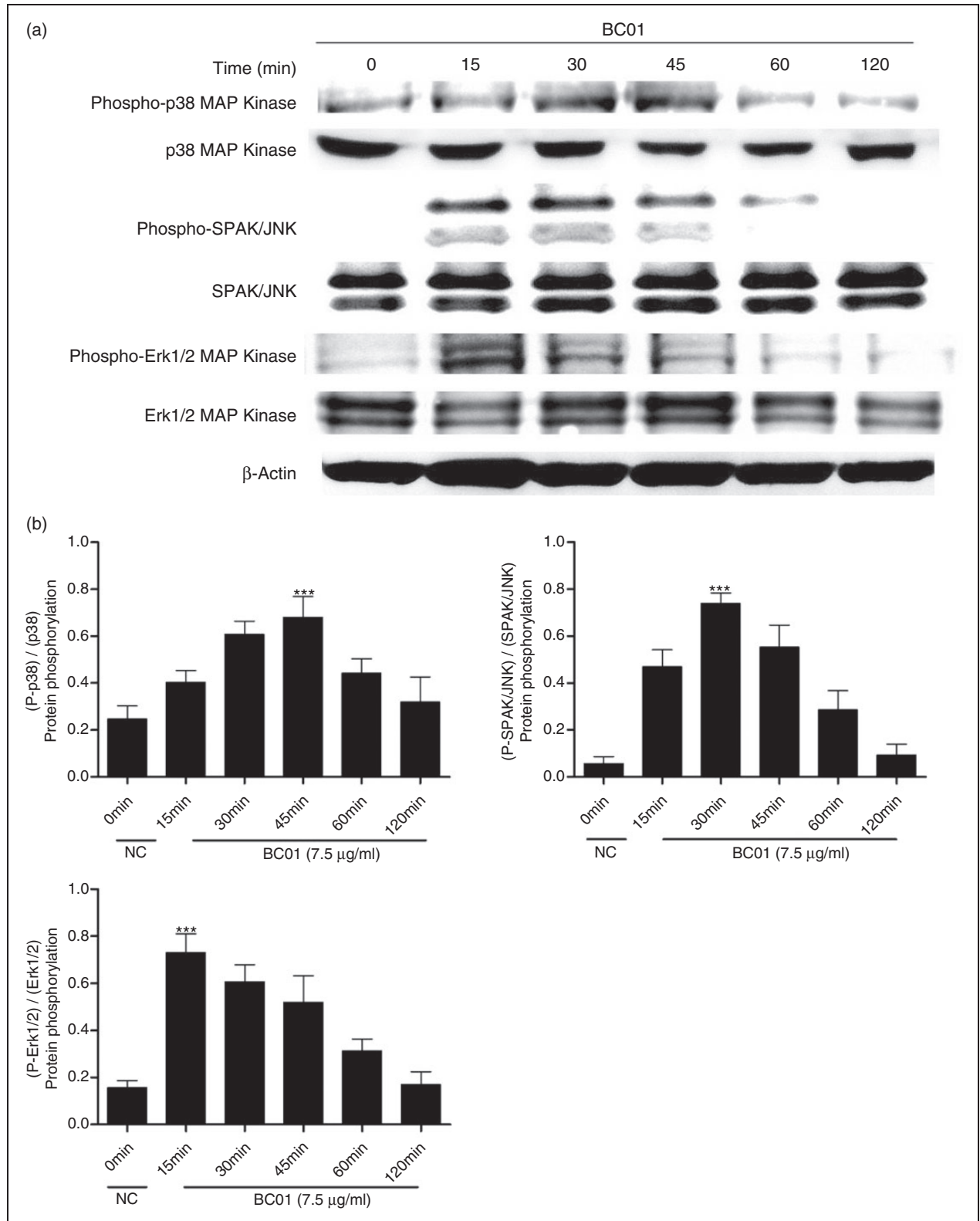


Figure 6. BC01 induces the phosphorylation of p38, SPAK/JNK, and Erk1/2. (a) RAW 264.7 cells were cultured in the presence of 7.5 μ g/ml of BC01 for 15, 30, 45, 60, or 120 min and Western blot analysis was used to examine the phosphorylation of p38, SPAK/JNK, and Erk1/2. T = 0 represents basal-level phosphorylation. Each specific Ab for the unphosphorylated kinase was used as a loading control. (b) Image J was used to quantify the intensity of the bands in phosphorylation of p38 (45min), SPAK/JNK (30 min) and Erk1/2 (15 min), protein phosphorylation intensity is expressed as the ratio phosphorylated protein/unphosphorylated protein. Data shown are expressed as the mean \pm SD from three independent experiments; NC, denotes negative control, *** $P < 0.001$.

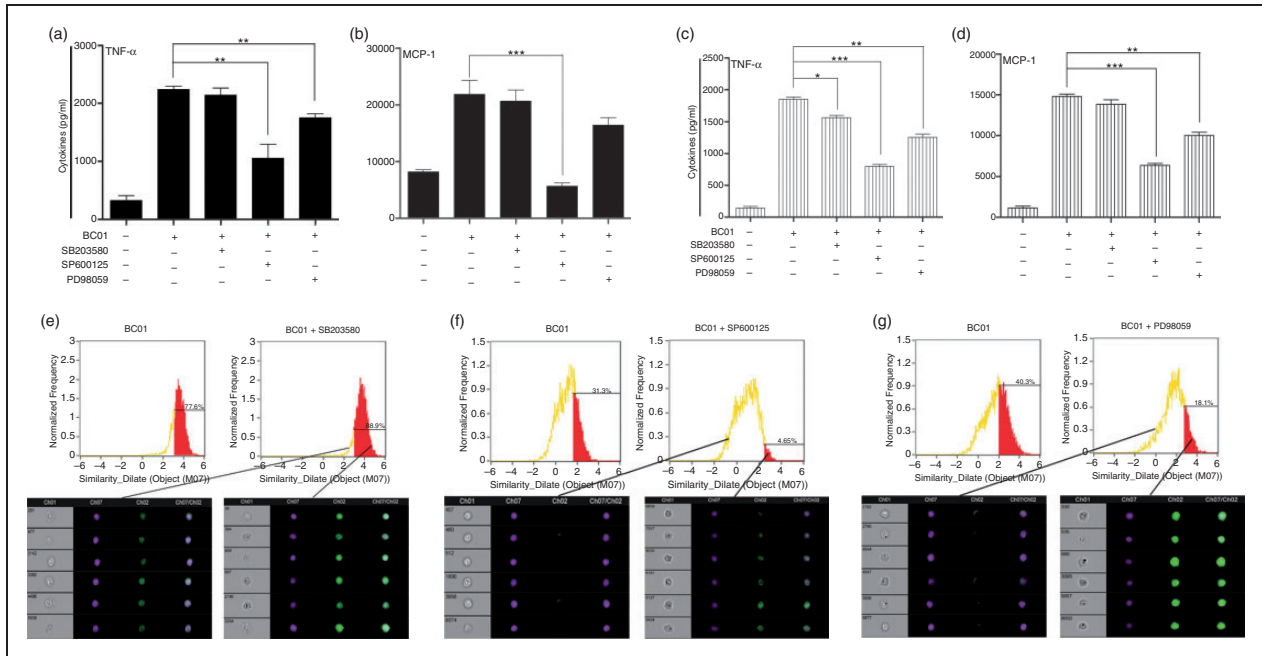


Figure 7. BC01 stimulates MAPKs activation and cytokine expression in murine macrophages. RAW 264.7 cells were pre- or post-treated with inhibitors (SB203580: 1 μ M, SP600125: 10 μ M, PD98059: 5 μ M, or ODN 2088: 2 μ M), and followed by stimulation with BC01. (a) and (b) RAW 264.7 cells were pre-treated with inhibitors for 12 h, followed by stimulation with 7.5 μ g/ml of BC01, the amounts of TNF- α and MCP-I were measured in the supernatants using ELISA. (c) and (d) RAW 264.7 cells were pre-treated with 7.5 μ g/ml of BC01 for 0.4 h, followed by incubation with inhibitors for 24 h. The levels of TNF- α and MCP-I were measured in the cell culture supernatants using ELISA. (e), (f), and (g) RAW 264.7 cells were cultured in the presence of BC01 for 45 min, stained and acquired with Image Stream 100. The left-side image shows the phosphorylation status of BC01-treated cells and the right-side image shows the phosphorylation status of BC01-treated cells after incubation with various MAPK pathway inhibitors. Bottom, from left to right, shown are the representative images of low or high phosphorylation (original magnification $\times 40$). Data shown are expressed as the mean \pm SD from three independent experiments. * $P < 0.05$, ** $P < 0.01$, *** $P < 0.001$.

same visual field revealed that the number of microspheres phagocytized by the peritoneal macrophages isolated from TLR9^{-/-} mice was significantly lower (mean: 7.6; $P < 0.01$), compared with that of C57BL/6 mice (mean: 14.1) (Figure 10(c)). These results indicate the involvement of TLR9 in BC01-induced macrophage phagocytosis.

BC01 induced expression of cell-surface molecules in macrophages in TLR9-mediated manner

Next, we investigated the effect of BC01 on the expression MHC-II, and cell-surface co-stimulatory molecules, such as CD40, CD80, and CD86 by murine macrophages. Cells were stimulated with 7.5 μ g/ml of BC01 for 12, 24, or 48 h, and analyzed by flow cytometry. Thus, BC01 stimulation of macrophages increased the expression of MHC-II by two folds at 24 and 48 h, compared with the control-stimulated cells ($P < 0.01$ and $P < 0.01$, Figure 11(a)). Similarly, stimulation of macrophages with BC01 significantly enhanced the expression of CD80 at 24 h ($P < 0.01$, Figure 11(c)); however, no significant effect was observed on the

expression of CD86 ($P > 0.05$, Figure 11(c)). Interestingly, the expression of CD40 peaked at 12 h, followed by gradual reduction until 48 h ($P < 0.01$ and $P < 0.01$, Figure 11(b)). Also, we have detected a significant up-regulation in the expression of MHC-II, CD40, CD80, and CD86 in BC01-treated peritoneal macrophages isolated from C57BL/6 (Figure 12(e), $P < 0.01$; Figure 12(f), $P < 0.01$; Figure 12(g), $P < 0.001$, and Figure 12(h), $P < 0.01$). These results suggested that BC01 can activate the immune response of macrophages by up-regulating the expression of MHC-II and other cell-surface co-stimulatory molecules.

To determine the role of TLR9 on BC01-mediated expression of MHC-II, CD40, CD80, and CD86 molecules, the RAW 264.7 were pre-treated with ODN 2088 and stimulated with BC01. The flow cytometry analysis of these cells showed an elevated expression of MHC-II and CD40 in the BC01 alone-stimulated cells, compared with the media control. Though ODN 2088 pre-treatment followed by BC01 stimulation also increased the expression of MHC-II and not CD40, the level of induction of these molecules in the ODN 2088 pre-treatment group was significantly lower

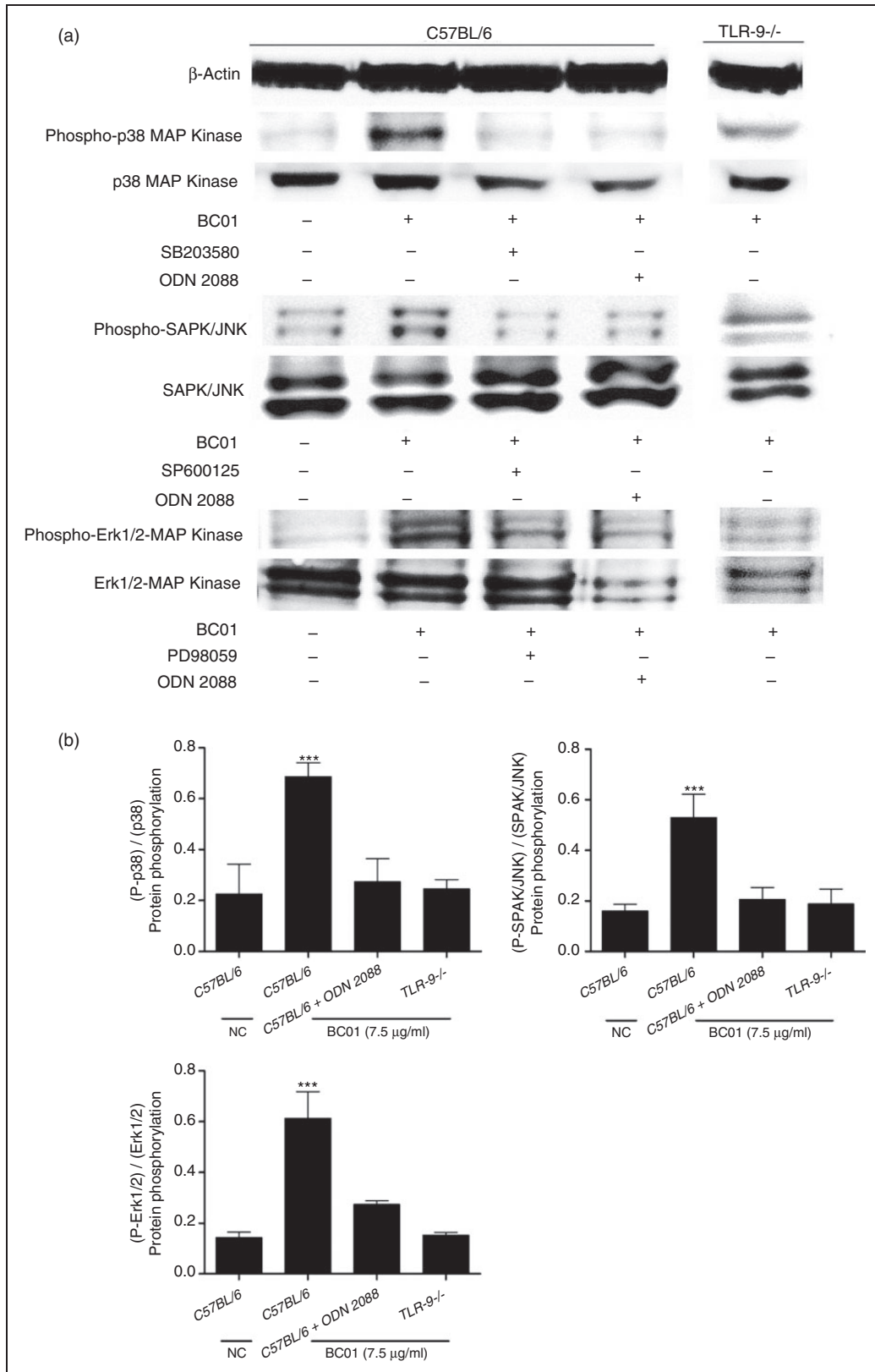


Figure 8. BC01 stimulates MAPKs activation through TLR9 in murine macrophages. (a) Murine peritoneal macrophages from wild type C57BL/6 or TLR9^{-/-} mice were cultured in the presence of 7.5 µg/ml of BC01 for 45, 30, and 15 min, and Western blot analysis was used to examine the phosphorylation of p38, SPAK/JNK, and Erk1/2. Each specific Ab for the unphosphorylated kinase was used as a loading control. (b) Image J is used to quantify the intensity of the bands in phosphorylation of p38 (45min), SPAK/JNK (30 min), and Erk1/2 (15 min), protein phosphorylation intensity is expressed as the ratio phosphorylated protein/unphosphorylated protein. Data shown are expressed as the mean ± SD from three independent experiments; NC denotes negative control. ***P < 0.001.

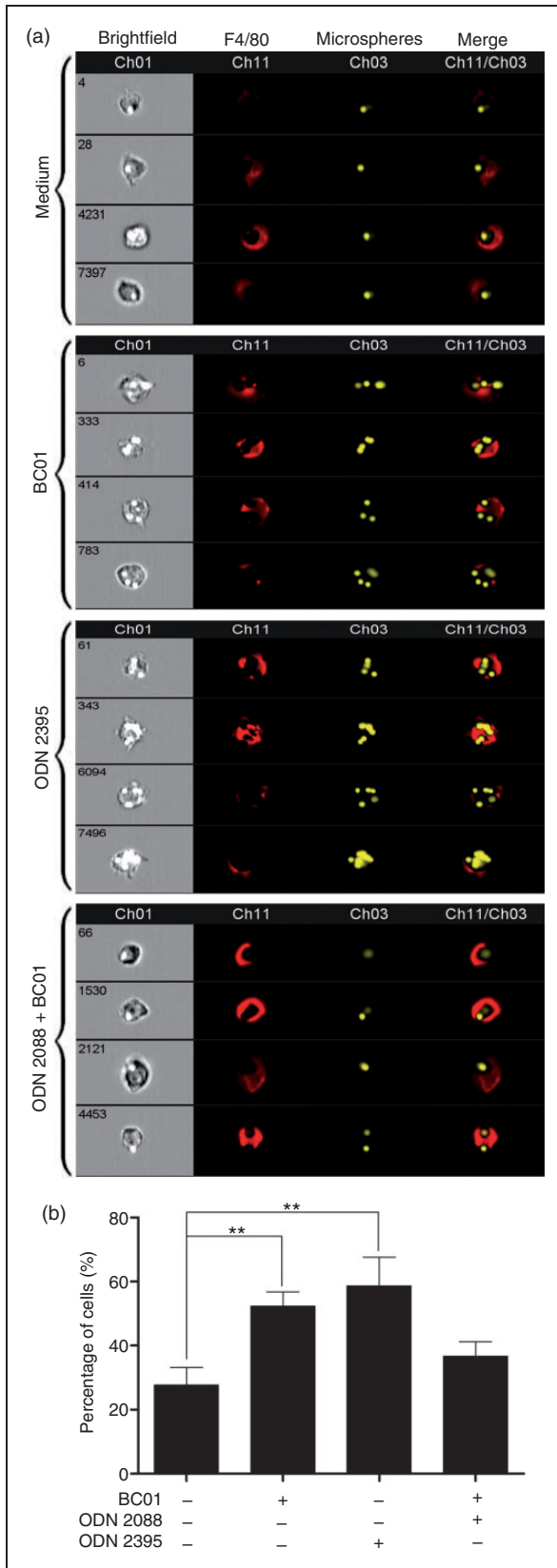


Figure 9. TLR9-mediated induction of phagocytosis by BC01 stimulated murine macrophages. RAW 264.7 cells were treated

than the cells treated with only BC01 (Figure 12(a), $P < 0.01$). No significant difference was noted in CD80 and CD86 between the control and BC01-stimulated, with or without ODN 2088 pre-treatment groups (Figure 12(c), $P > 0.05$, and Figure 12(d), $P > 0.05$). However, results obtained with primary macrophages were slightly different than those obtained with murine cell lines. Importantly, the expression levels of MHC-II, CD40, CD80, and CD86 molecules were significantly reduced in the peritoneal macrophages of TLR9^{-/-} mice, compared with the wild type C57BL/6 mice (Figure 12(e), $P < 0.001$, Figure 12(f), $P < 0.001$, Figure 12(g), $P < 0.001$, and Figure 12(h), $P < 0.01$). These results suggest that TLR9 plays a role in BC01-mediated induction of MHC-II and co-stimulatory molecules expression, and also highlights the subtle variations in the pattern of expression of these molecules between primary cells and cell lines.

BC01 induced inflammatory cytokine expression in a TLR9-dependent manner in mice

Inflammatory cytokines, such as TNF- α , IFN- γ , IL-6, and IL-17 activate immune cells including APCs and lymphocytes, regulate the metabolic activities of these cells, promote the synthesis and release of other cytokines, and play an essential role in regulating the host immunity. As TLR9 is a critical receptor in the APC and as BC01-mediated APC activation involves TLR9, we wanted to determine the contribution of TLR9 on the BC01-mediated host immune activities. As shown in Figure 13(a), wild type C57BL/6, and TLR9^{-/-} mice were injected with BC01; 3 d after the final injection animals were necropsied, and the levels of inflammatory cytokines/chemokines were determined in the serum. As shown in Figure 13(b), BC01-injected C57BL/6 mice showed significantly higher levels of all the tested inflammatory cytokines/chemokines, except for IL-1 α , in the serum, whereas the levels of the same cytokines were remarkably attenuated in TLR9^{-/-}

Figure 9. Continued.

with or without BC01, ODN2395 or a TLR9 antagonist, ODN 2088 for 12 h, and the cells were co-cultured with fluorescent microspheres at 37°C for 2 h. After washing with sterile PBS, cells were labeled with APC-F4/80 Ab and evaluated using Amnis Image Stream Data Analysis. (a) Representative images after Amnis acquisition (original magnification $\times 40$, 10000 events per condition) showing different extents of phagocytosis during various treatment conditions. (b) Image Stream data were acquired using the Amnis Image Stream Analyzer, and the percentage of macrophages that internalized microspheres was quantitated using the Amnis IDEAS software. Data shown are mean \pm SD from at least three independent experiments, ** $P < 0.01$.

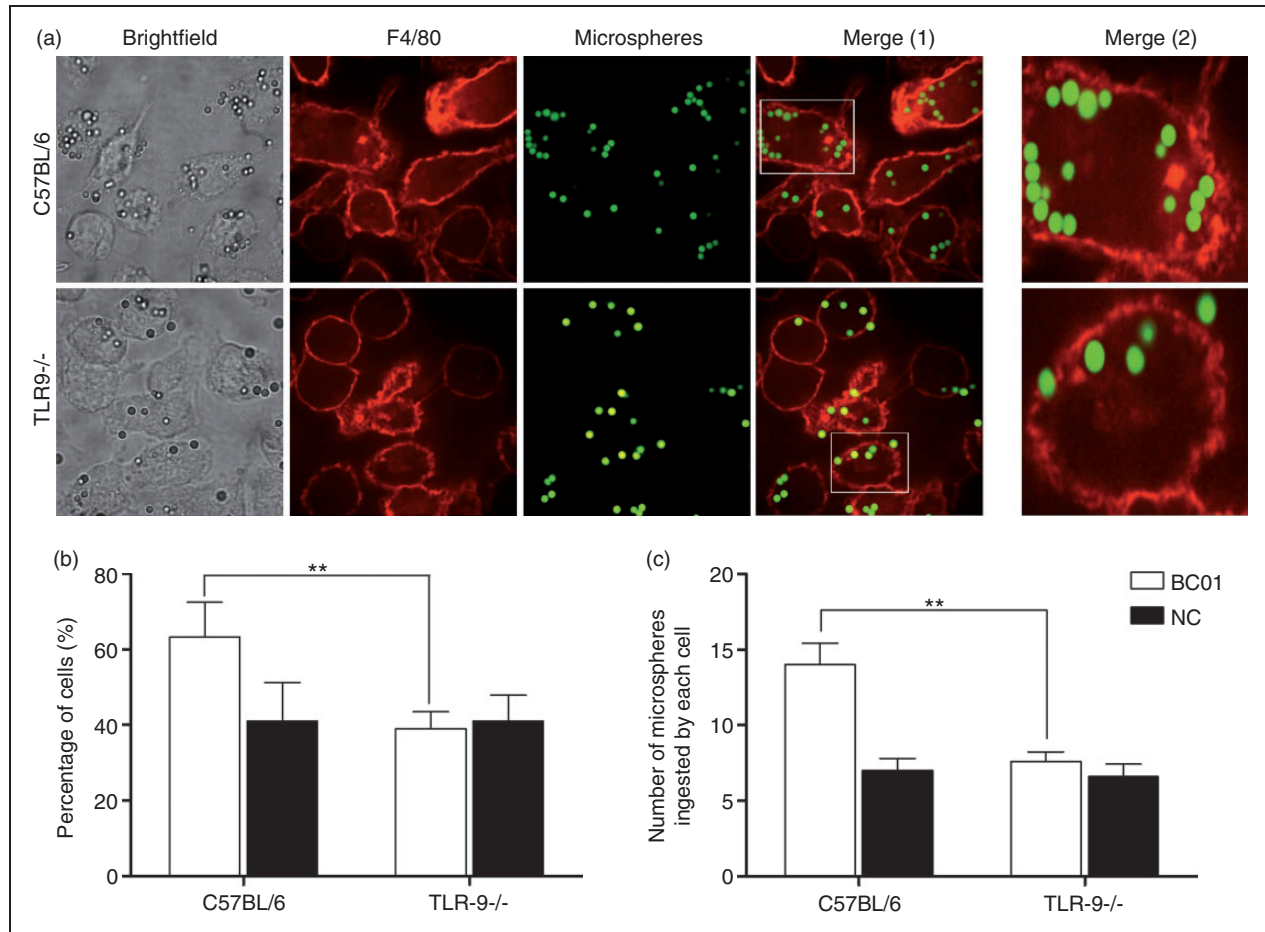


Figure 10. Phagocytosis by peritoneal macrophages from wild type C57BL/6 or TLR9^{-/-} mice after stimulation with BC01. Peritoneal macrophages from wild type C57BL/6 or TLR9^{-/-} mice were stimulated with BC01 and incubated with fluorescent microspheres at 37°C for 2 h. After washing with sterile PBS, macrophages were labeled with APC-F4/80 Ab, and confocal microscopy was used to analyze phagocytosis. (a) Representative images after laser scanning confocal microscopy acquisition (original magnification $\times 100$, oil immersion objective) showing differential phagocytosis by peritoneal macrophages from the wild type or TLR9^{-/-} mice. (b) Confocal microscopy-assisted enumeration of macrophages that consumed at least one fluorescent microsphere. (c) Confocal microscopy-assisted count of fluorescent microspheres internalized by individual cells. Each experiment calculated at least 100 cells in at least 10 visual fields. For (b) and (c), the data shown are mean \pm SD from at least three independent experiments. NC denotes negative control; ** $P < 0.01$.

mice. Expression of IL-1 α was elevated in the TLR9^{-/-} mice compared with the wild type. These results indicate that BC01-mediated induction of inflammatory cytokines/chemokines is dependent, at least in part, on TLR9. These *in vivo* findings also reinforce the vital role of TLR9 in BC01-induced activation of the innate immune system.

TLR9 is required for BC01-induced APC proliferation

As part of the host's innate immune system, APCs are crucial for the effective control of infectious disease in humans and other experimental animals. We noticed that BC01 stimulated APC function *in vitro* and *ex*

in vivo in a TLR9-dependent manner. We also observed elevated levels of pro-inflammatory cytokines/chemokines in BC01-immunized mice that were dependent on TLR9. To determine the impact of these changes on the immune cell distribution *in vivo*, we measured the B lymphocytes, dendritic cells, and macrophages in the single-cell suspensions prepared from the lymph nodes of BC01-immunized mice using flow cytometry (Table 1). The obtained results showed that the percentage of APCs was significantly increased in both wild type and TLR9^{-/-} mice after three doses of immunization with BC01. In addition, the percentages of B lymphocytes (32.3%) and macrophages (2.4%) were significantly increased in the lymph nodes of

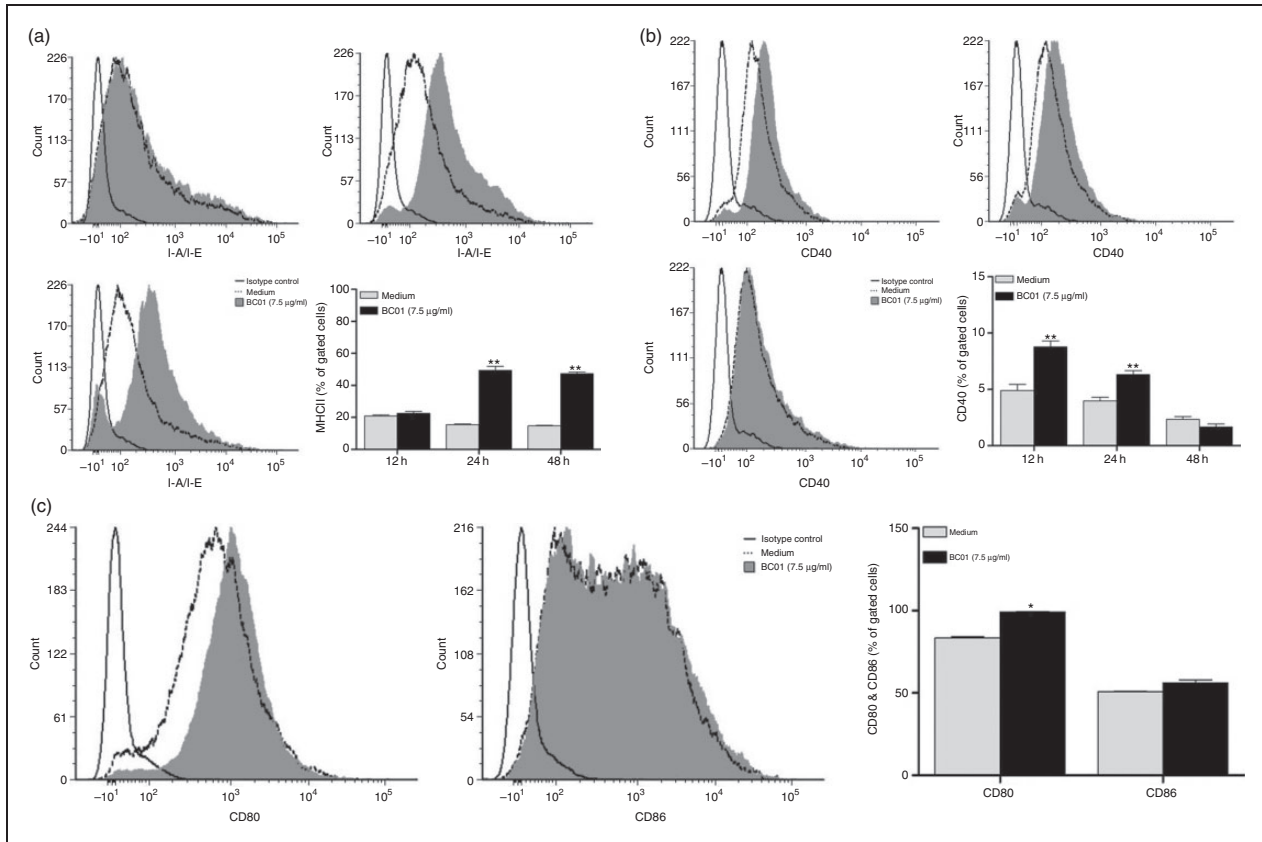


Figure 11. BC01 up-regulates the expression of MHC-II and cell-surface co-stimulatory molecules in murine macrophages. (a) Flow cytometry measurement of MHC-II expression on the RAW 264.7 cell surface after stimulation with 7.5 µg/ml of BC01 for 12 h, 24 h, or 48 h. (b) Flow cytometry measurement of cell-surface CD40 expression on RAW 264.7 cells after stimulation with 7.5 µg/ml of BC01 for 12 h, 24 h, or 48 h. (c) Flow cytometry measurement of cell-surface CD80 and CD86 expression on RAW 264.7 cells after stimulation with 7.5 µg/ml of BC01 for 24 h. Data shown are mean \pm SD from three independent experiments. * $P < 0.05$, ** $P < 0.01$.

C57BL/6 mice, compared with the TLR9^{-/-} mice, 28.6% and 1.0% respectively, ($P < 0.05$ and $P < 0.05$, Table 1). However, no significant effect of immunization with BC01 was observed on the percentage of dendritic cells in any of the groups ($P > 0.05$ and $P > 0.05$, Table 1).

Discussion

The innate immune response plays an essential role in the non-specific, anti-infective immunity of the host and the initiation, regulation, and effector phases of a more specific, adaptive immune response. Therefore, the ability to optimally activate the innate immune response has been one of the critical indicators for evaluating the performance of vaccines and adjuvants.

Engagement of TLRs by exogenous and endogenous signaling molecules, such as PAMPs and DAMPs, respectively, leads to activation of macrophage effector functions, which play crucial roles in regulating the host innate and adaptive immunity during disease

conditions. In the present study, we showed that the activation of murine macrophages with an adjuvant, BC01, significantly increased the production of TNF- α and MCP-1. In addition, the loss of macrophage-stimulating activity of BC01 after digestion with DNase I indicates that BC01-induced production of pro-inflammatory cytokines was not due to the presence of proteins or polysaccharides, but rather a specific property of the unmethylated CpG motif-containing DNA fragments extracted from BCG genome. Consistent with Diesel et al., our data suggest that binding of BCG DNA to TLR receptors is a key signaling event that induces cytoskeletal changes and associated macrophage cell activation.³⁹ However, the precise mode of action of TLR agonists (BC01, ODN 2395) and antagonists (ODN 2088) and the structural requirement of these molecules in stimulating TLR signaling and subsequently inducing pro-inflammatory molecules remains unknown. Unraveling the mechanism of action of TLR agonists/antagonists and comparing their nanoparticulate structures associated with

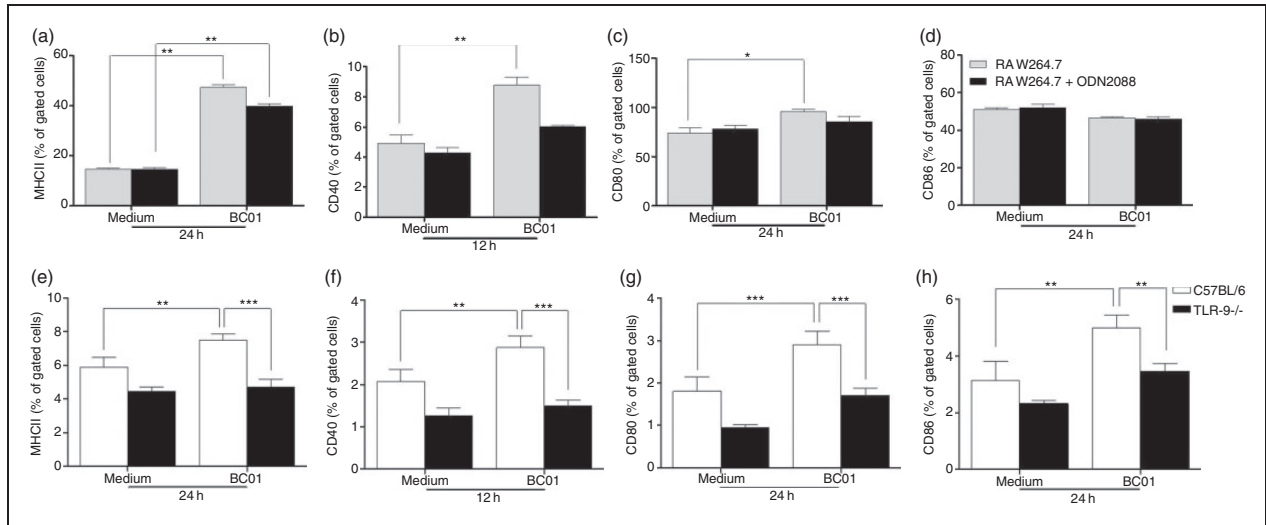


Figure 12. TLR9-dependent up-regulation of MHC-II and cell-surface co-stimulatory molecules during BC01 stimulation of murine macrophages. (a–d) RAW 264.7 cells were treated with or without TLR9 antagonist, ODN 2088 for 12 h, followed by stimulation with 7.5 μ g/ml of BC01 and then flow cytometry was used to measure MHC-II, CD40, CD80, and CD86 expression on the cells. (e–h) Flow cytometric measurement of MHC-II, CD40, CD80, and CD86 expression on the cell surface of peritoneal macrophages from C57BL/6 or TLR9^{-/-} mice after stimulation with 7.5 μ g/ml of BC01. Data shown are mean \pm SD from three independent experiments. * P < 0.05, ** P < 0.01, *** P < 0.001.

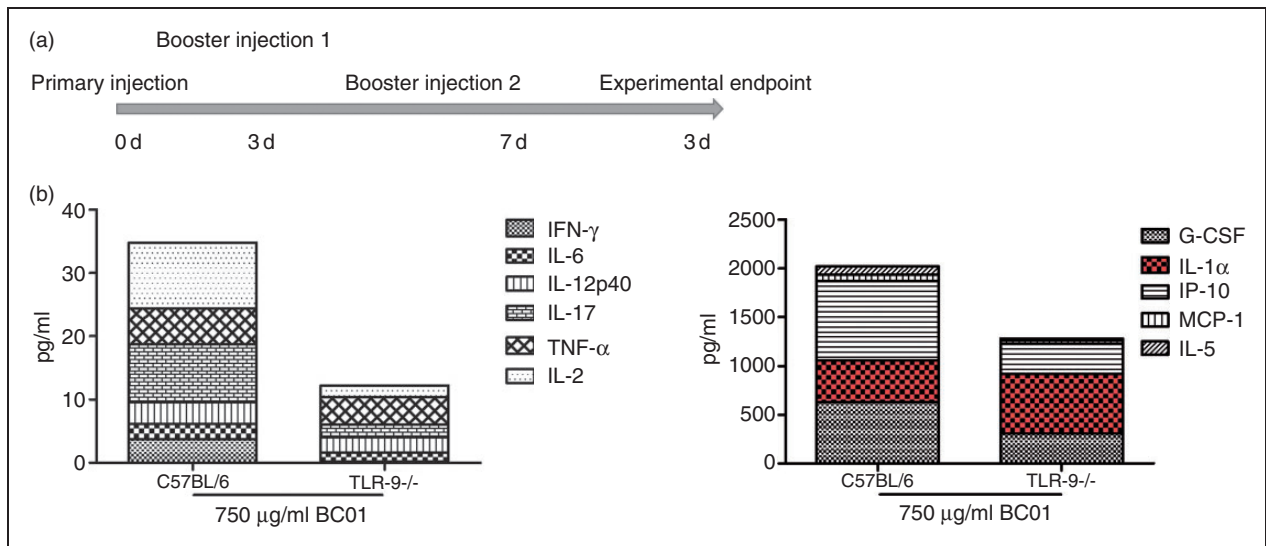


Figure 13. Injection of wild type C57BL/6 or TLR9^{-/-} mice with BC01 differentially alters the systemic cytokine levels. (a) Schema of the C57BL/6 or TLR9^{-/-} mice injection experiment showing the schedule. (b) Quantitative detection of inflammatory cytokines in mice. Three days after the final immunization, mice were necropsied, and serum cytokines levels were measured by the MILLIPLEX[®] MAP Kit. IL-1 α levels in TLR9^{-/-} mice were significantly higher than in C57BL/6 mice, shown in red.

induction of large amounts of TNF- α is worth further exploration. Such studies can help to devise better immune-stimulatory molecules.⁴⁰

TLR-mediated signaling pathways predominately activate NF- κ B, which is a critical transcription factor that regulates the gene expression during the innate and adaptive immune responses.^{41,42} Engagement of TLRs

by cognate ligands ultimately activates NF- κ B, which translocates from the cytoplasm into the nucleus and modulates the expression of genes involved in the immune responses.^{43,44} In this study, we showed significant induction in the nuclear translocation of NF- κ B p65. This observation is consistent with the induction of pro-inflammatory cytokines, such as

Table 1. APCs composition in mice lymph nodes.

	C57BL/6		TLR9 ^{-/-}	
	PBS	BC01	PBS	BC01
B Lymphocyte	22.5 ± 5.1	32.3 ± 5.3	23.6 ± 2.3	28.6 ± 4.7
Dendritic cells	2.3 ± 0.4	2.5 ± 0.4	3.1 ± 0.5	2.9 ± 0.7
Macrophage	0.9 ± 0.3	2.4 ± 0.3	0.9 ± 0.2	1.0 ± 0.2

Flow cytometry was used to determine the percentage of various APCs in the single-cell suspensions of lymph nodes from wild type and TLR9^{-/-} mice (10,000 events per condition). Data shown are mean ± SD.

Numbers in **bold italics** have a $P < 0.05$.

TNF- α and MCP-1. These activities were inhibited significantly when BC01 was co-incubated with JSH-23, which indicates the BC01 induced the NF- κ B p65 nuclear translocation, which in turn activated the NF- κ B signal pathway, and promoted pro-inflammatory cytokine secretion.

In mammalian cells, the structure of NF- κ B structure consists of five homologous subunits, and all NF- κ B family members have a Rel homology domain, which is necessary for homo- and heterodimerization, nuclear localization, and DNA and I κ B α binding.^{43,45} NF- κ B works as dimers formed by the interactions of two of the five Rel family proteins.⁴⁶ Recently, the phosphorylation and acetylation of p65 were shown to be crucial for DNA binding and transactivation of NF- κ B.⁴⁷⁻⁴⁹ In addition, a shift in NF- κ B subunits from p50-p65 to p50 homodimers has been shown to be associated with the resolution of inflammation,⁵⁰ and IKK has also been reported to phosphorylate NF- κ B p65.^{48,51} Our study showed that stimulation of macrophages with BC01 or ODN 2395 significantly increased the phosphorylation levels of NF- κ B p65, NF- κ B p105/p50, and NF- κ B p100/p52 molecules which are components of the NF- κ B pathway. Thus, we confirm that the macrophage stimulation of BC01 involves activation of the NF- κ B signaling pathway.

TLR9 is the only endosomal PRR that mediates potent innate response, specifically to bacterial and viral DNA.⁵² TLR9 preferentially recognizes DNA sequence motifs containing the CpG dinucleotide. Synthetic ODNs, such as ODN 2395 used in this study, have been studied previously as adjuvants either as soluble, nanoparticle formulations⁵³ or as virus-like particles.⁵⁴ Previous studies have shown that synthetic ODNs containing unmethylated CpG motifs activate cells that express TLR9 to mount an innate immune response, characterized by the production of pro-inflammatory Th1 cytokines mediated by NF- κ B signaling.⁵⁵ Besides, DNA isolated from *M. tuberculosis* H37Ra and *M. bovis* BCG activates macrophages via TLR9 signaling to mount an

antibacterial response against MTB in human and murine alveolar macrophages.⁵⁶ Moreover, a fraction complex extracted from *M. bovis* BCG, which contained more than 90% of nucleic acids and less than 2% of bacterial proteins, was found to possess intense antitumor activity in murine and guinea pig models.^{57,58} Although these studies highlighted the immune-stimulatory activities of mycobacterial nucleic acids through TLR9 signaling, the methylation status of the stimulant used was not described. Similarly, no immune-regulatory studies have been performed previously using BC01, which are unmethylated, CpG motif-containing DNA fragments derived from the genome of BCG as described in this study.

In addition to NF- κ B, the MAPKs pathway is another signaling cascade that regulates immune response to external stimuli. In mammalian cells, the MAPK system comprises a family of protein-serine or threonine kinases. The p38, SPAK/JNK, and Erk1/2 kinases link the extracellular signals from activated receptors, located in the plasma membrane, to the nucleus. This signal initiates various cellular responses such as cell proliferation and differentiation, survival, death, and apoptosis.^{31,59,60} Studies have shown that infection of macrophages by *M. tuberculosis* complex⁶¹⁻⁶³ or *Mycobacterium avium*⁶⁴ activates the MAPKs signaling cascade to protect the host from the invasion/survival of these pathogens. Phosphorylation of molecules involved in the MAPKs signaling pathway ultimately results in the expression of pro-inflammatory cytokines. Our studies indicate that BC01 stimulation of macrophages can activate SPAK/JNK and Erk1/2 that can induce TNF- α and MCP-1 expression via the TLR9 pathway. Further, specific inhibitors in this pathway significantly attenuated the phosphorylation of SPAK/JNK and Erk1/2 kinases, and ultimately reduced the expression of TNF- α and MCP-1 in the RAW 264.7 cells. In addition, the levels of phosphorylated p38, SPAK/JNK, and Erk1/2 were increased in the RAW 264.7 cells following the BC01 stimulation. Consistently, low, basal-level phosphorylation was observed in the peritoneal macrophages of C57BL/6 mice that were pre-treated with p38, SPAK/JNK, or Erk1/2 inhibitors. Moreover, the MAPK-mediated pro-inflammatory cytokine induction was abolished in RAW 264.7 cells, when TLR9 inhibitor was added along with BC01 in the culture, and the peritoneal macrophages obtained from TLR9^{-/-} mice. Taken together, our findings suggested that BC01 stimulation is capable of activating several innate immune signaling pathways in murine macrophages, by primarily engaging TLR9, which culminates in the elevated pro-inflammatory cytokine production.

Among various innate immune responses, macrophage-mediated phagocytosis is a crucial process to remove pathogens^{65,66} and cell debris.⁶⁷ Therefore, the ability to enhance macrophage function has become an important indicator to assess the performance of adjuvants that are capable of stimulating innate immunity. In this study, we evaluated BC01 ability to enhance the phagocytic activity of macrophages, and our results indicated that BC01 and ODN 2395 could significantly improve phagocytosis by macrophages from 27.7% (untreated) to 52.3% (BC01) and 58.7% (ODN 2395). However, when the macrophages were pre-treated with a TLR9 antagonist, their phagocytic activity was significantly decreased. These results were also consistent with similar experiments performed using primary cells, in which we observed that BC01 enhanced the phagocytic activity of peritoneal macrophages in a TLR9 pathway-dependent manner. Consistent with these phagocytosis experiments, BC01 stimulation of macrophages increased the expression of MHC-II and cell-surface co-stimulating molecules in a TLR9-mediated manner. This phenomenon was also confirmed in experiments performed with peritoneal macrophages from C57BL/6 and TLR9^{-/-} mice.

In our studies, the purpose of *in vivo* experiments in mice was to verify and extend our *in vitro* findings that BC01 treatment can activate a signaling pathway that induces pro-inflammatory chemokines and cytokines in mice. In addition, we used TLR9 knockout mice to show that the BC01-mediated immune changes on the host are associated with TLR9.

In the pilot experiments, we have studied the expression levels of various cytokines in mice at different time points after single-dose administration of BC01 (Figure S4). Surprisingly, we found that a single dose was not sufficient to stimulate the TLR9 knockout mice to mount an immune response. In addition, a previous study has shown that BC01 treatment promotes the proliferation of mouse T and B lymphocytes, enhances NK cell killing activity, increases the content of CD3⁺, CD4⁺, and CD8⁺ T cells in the spleen, and restores the immune function of T and B lymphocytes in the immune-compromised animals.⁶⁸ Therefore, it appears that, in addition to acting as a vaccine adjuvant, BC01 can also function as an immunomodulatory molecule. Based on this knowledge, we performed a booster dose to test if we can improve the immune response induced by BC01. However, as shown in Figure 13(b), the cascade of systemic pro-inflammatory cytokines produced by booster stimulation with BC01 was significantly lower in the TLR9^{-/-} compared with the wild type mice, which further proves that TLR9 function is essential for the BC01-mediated activation of the host innate immune response. In addition, evaluation of the composition of

APCs in the lymph node of mice indicated that BC01 stimulation significantly induces B lymphocyte and macrophage proliferation in the wild type C57BL/6 mice compared with the TLR9^{-/-} mice.

In conclusion, our study demonstrates that BC01 is a potent TLR9 agonist, induces innate immunity, and up-regulates the production of pro-inflammatory cytokines upon stimulation of macrophages *in vitro* or *ex vivo*, and in a mouse model of *in vivo* stimulation. We also show that the innate immune activation properties of BC01 involve NF- κ B and MAPKs signaling pathways. These observations provide a better understanding of the immunoregulatory mechanisms of BC01 that is vital to accelerate the clinical utility of this molecule to boost innate host immunity against invading pathogens.

Acknowledgements

The authors are grateful to professor Jun Zhou of Institute of Basic Medical Sciences, Chinese Academy of Medical Sciences & Peking Union Medical College for assisting in the use of Ultra VIEW Vox-3D Live Cell Imaging System and Amnis Image Stream 100.

Declaration of conflicting interests

The author(s) declared no potential conflicts of interest with respect to the research, authorship and/or publication of this article.

Funding

The author(s) received no financial support for the research, authorship and/or publication of this article.

ORCID iD

Junli Li  <https://orcid.org/0000-0001-5542-3375>

Supplemental material

Supplemental material is available for this article online.

References

1. McKee AS, Munks MW and Marrack P. How do adjuvants work? Important considerations for new generation adjuvants. *Immunity* 2007; 27: 687–690.
2. McCartney S, Vermi W, Gilfillan S, et al. Distinct and complementary functions of MDA5 and TLR3 in poly(I:C)-mediated activation of mouse NK cells. *J Exp Med* 2009; 206: 2967–2976.
3. O'Hagan DT and De Gregorio E. The path to a successful vaccine adjuvant—the long and winding road'. *Drug Discov Today* 2009; 14: 541–551.
4. McKee AS, MacLeod MK, Kappler JW, et al. Immune mechanisms of protection: Can adjuvants rise to the challenge? *BMC Biol* 2010; 8: 37.

5. Medzhitov R, Preston-Hurlburt P and Janeway CA Jr. A human homologue of the Drosophila Toll protein signals activation of adaptive immunity. *Nature* 1997; 388: 394–397.
6. Aderem A and Ulevitch RJ. Toll-like receptors in the induction of the innate immune response. *Nature* 2000; 406: 782–787.
7. Zhang G and Ghosh S. Toll-like receptor-mediated NF- κ B activation: A phylogenetically conserved paradigm in innate immunity. *J Clin Invest* 2001; 107: 13–19.
8. Takeda K, Kaisho T and Akira S. Toll-like receptors. *Annu Rev Immunol* 2003; 21: 335–376.
9. Iwasaki A and Medzhitov R. Toll-like receptor control of the adaptive immune responses. *Nat Immunol* 2004; 5: 987–995.
10. Doyle SL and O'Neill LAJ. Toll-like receptors: From the discovery of NF κ B to new insights into transcriptional regulations in innate immunity. *Biochem Pharmacol* 2006; 9: 1102–1113.
11. Kawai T and Akira S. Toll-like receptors and their crosstalk with other innate receptors in infection and immunity. *Immunity* 2011; 34: 637–650.
12. Matzinger P. Tolerance, danger, and the extended family. *Annu Review Immunol* 1994; 12: 991–1045.
13. Rakoff-Nahoum S, Paglino J, Eslami-Varzaneh F, et al. Recognition of commensal microflora by toll-like receptors is required for intestinal homeostasis. *Cell* 2004; 2: 229–241.
14. Adams S. Toll-like receptor agonists in cancer therapy. *Immunotherapy-UK* 2009; 1: 949–964.
15. Casella CR and Mitchell TC. Putting endotoxin to work for us: Monophosphoryl lipid A as a safe and effective vaccine adjuvant. *Cell Mol Life Sci* 2008; 65: 3231.
16. Didierlaurent AM, Morel S, Lockman L, et al. AS04, an aluminum salt- and TLR4 agonist-based adjuvant system, induces a transient localized innate immune response leading to enhanced adaptive immunity. *J Immunol* 2009; 183: 6186–6197.
17. Krieg AM, Yi AK, Matson S, et al. CpG motifs in bacterial DNA trigger direct B-cell activation. *Nature* 1995; 374: 546–549.
18. Krieg AM. Therapeutic potential of Toll-like receptor 9 activation. *Nat Rev Drug Discov* 2006; 5: 471–484.
19. Kumagai Y, Takeuchi O and Akira S. TLR9 as a key receptor for the recognition of DNA. *Adv Drug Deliver Reviews* 2008; 60: 795–804.
20. Gupta G and Agrawal D. CpG oligodeoxynucleotides as TLR9 agonists: Therapeutic application in allergy and asthma. *BioDrugs* 2010; 24: 225–235.
21. Blasius AL and Beutler B. Intracellular toll-like receptors. *Immunity* 2010; 32: 305–315.
22. Kobayashi H, Horner AA, Takabayashi K, et al. Immunostimulatory DNA pre-priming: A novel approach for prolonged Th1-biased immunity. *Cell Immunol* 1999; 198: 69–75.
23. Tighe H, Takabayashi K, Schwartz D, et al. Conjugation of immunostimulatory DNA to the short ragweed allergen amb a 1 enhances its immunogenicity and reduces its allergenicity. *J Allergy Clin Immunol* 2000; 106: 124–134.
24. Hou B, Reizis B and DeFranco AL. Toll-like receptors activate innate and adaptive immunity by using dendritic cell-intrinsic and -extrinsic mechanisms. *Immunity* 2008; 29: 272–282.
25. Campbell JD, Cho Y, Foster ML, et al. CpG-containing immunostimulatory DNA sequences elicit TNF- α -dependent toxicity in rodents but not in humans. *J Clin Invest* 2009; 119: 2564–2576.
26. Reiling N, Blumenthal A, Flad HD, et al. Mycobacteria-induced TNF- and IL-10 formation by human macrophages is differentially regulated at the level of mitogen-activated protein kinase activity. *J Immunol* 2001; 167: 3339–3345.
27. Medzhitov R. Toll-like receptors and innate immunity. *Nat Rev Immunol* 2001; 1: 135–145.
28. Rakoff-Nahoum S and Medzhitov R. Toll-like receptors and cancer. *Nat Reviews Cancer* 2009; 9: 57–63.
29. Karin M and Greten FR. NF- κ B: Linking inflammation and immunity to cancer development and progression. *Nat Rev Immunol* 2005; 5: 749–759.
30. Nick JA, Avdi NJ, Gerwins P, et al. Activation of a p38 mitogen-activated protein kinase in human neutrophils by lipopolysaccharide. *J Immunol* 1996; 156: 4867–4875.
31. Lee JC, Laydon JT, McDonnell PC, et al. A protein kinase involved in the regulation of inflammatory cytokine biosynthesis. *Nature* 1994; 372: 739–746.
32. Scharf S, Hippenstiel S, Flieger A, et al. Induction of human beta-defensin-2 in pulmonary epithelial cells by *Legionella pneumophila*: involvement of TLR2 and TLR5, p38 MAPK, JNK, NF- κ B, and AP-1. *Am J Physiol-Lung C* 2010; 298: L687–L695.
33. Mellett M, Atzei P, Jackson R, et al. Mal mediates TLR-induced activation of CREB and expression of IL-10. *J Immunol* 2011; 186: 4925–4935.
34. Thapa B, Kim YH, Kwon HJ, et al. Novel regulatory mechanism and functional implication of plasminogen activator inhibitor-1 (PAI-1) expression in CpG-ODN-stimulated macrophages. *Mol Immunol* 2012; 49: 572–581.
35. Zhao AH, Qiao LY, Jia SZ, et al. Effect of BCG-CpG-DNA as an immunoadjuvants of recombinant HBsAg. *Chin J Biol* 2007; 5: 356–358 + 361.
36. Zhao AH, Li FX, Jia SZ, et al. Immunoadjuvants activity of BCG-CpG-DNA on group A meningococcal polysaccharide vaccine. *Chin Med Biotechnol* 2010; 2: 94–97.
37. Chen L, Xu M, Wang ZY, et al. The development and preliminary evaluation of a new *Mycobacterium tuberculosis* vaccine comprising Ag85b, HspX and CFP-10: ESAT-6 fusion protein with CpG DNA and aluminum hydroxide adjuvants. *Fems Immunol Med Mic* 2010; 59: 42–52.
38. Zhang Y, Yang YC, Zhang J, et al. Immune effect of STAg combined with BCG-DNA and aluminum hydroxide in mice. *Chin J Biol* 2011; 24: 1177–1179.
39. Diesel B, Hoppstädter J, Hachenthal N, et al. Activation of Rac1 GTPase by nanoparticulate structures in human macrophages. *Eur J Pharm Biopharm* 2013; 84: 315–324.
40. Kerkmann M, Costa LT, Richter C, et al. Spontaneous formation of nucleic acid-based nanoparticles is

- responsible for high interferon- α induction by CpG-A in plasmacytoid dendritic cells. *J Biol Chem* 2005; 280: 8086–8093.
41. Porter AG and Jänicke RU. Emerging roles of caspase-3 in apoptosis. *Cell Death Differ* 1999; 6: 99–104.
 42. Ashall L, Horton CA, Nelson DE, et al. Pulsatile stimulation determines timing and specificity of NF- κ B-dependent transcription. *Science* 2009; 324: 242–246.
 43. Baldwin AS, Jr. The NF- κ B and I κ B proteins: new discoveries and insights. *Annu Rev Immunol* 1996; 14: 649–683.
 44. Ghosh S, May M and Kopp E. NF- κ B and Rel proteins: Evolutionarily conserved mediators of immune responses. *Annu Rev Immunol* 1998; 16: 225–260.
 45. Ghosh S and Karin M. Missing pieces in the NF- κ B puzzle. *Cell* 2002; 109: S81–S96.
 46. Akira S and Takeda K. Toll-like receptor signalling. *Nat Rev Immunol* 2004; 4: 499–511.
 47. Egan LJ, Mays DC, Huntoon CJ, et al. Inhibition of interleukin-1-stimulated NF- κ B RelA/p65 phosphorylation by mesalamine is accompanied by decreased transcriptional activity. *J Biol Chem* 1999; 274: 26448–26453.
 48. Sakurai H, Chiba H, Miyoshi H, et al. I κ B kinases phosphorylate NF- κ B p65 subunit on serine 536 in the transactivation domain. *J Biol Chem* 1999; 274: 30353–30356.
 49. Chen L, Fischle W, Verdin E, et al. Duration of nuclear NF- κ B action regulated by reversible acetylation. *Science* 2001; 293: 1653–1657.
 50. Lawrence T, Gilroy DW, Colville-Nash PR, et al. Possible new role for NF- κ B in the resolution of inflammation. *Nat Med* 2001; 7: 1291–1297.
 51. Sizemore N, Lerner N, Dombrowski N, et al. Distinct roles of the I κ B kinase alpha and beta subunits in liberating nuclear factor kappa B (NF- κ B) from I κ B and in phosphorylating the p65 subunit of NF- κ B. *J Biol Chem* 2002; 277: 3863–3869.
 52. Blasius AL and Beutler B. Intracellular toll-like receptors. *Immunity* 2010; 32: 305–315.
 53. Marshall JD, Higgins D, Abbate C, et al. Polymyxin B enhances ISS-mediated immune responses across multiple species. *Cell Immunol* 2004; 229: 93–105.
 54. Jennings GT and Bachmann MF. Immunodrugs: Therapeutic VLP-based vaccines for chronic diseases. *Annu Rev Pharmacol* 2009; 49: 303–326.
 55. Bode C, Zhao G, Steinhagen F, et al. CpG DNA as a vaccine adjuvant. *Expert Rev Vaccines* 2011; 10: 499–511.
 56. Kiemer AK, Senaratne RH, Hoppstädter J, et al. Attenuated activation of macrophage TLR9 by DNA from virulent mycobacteria. *J Innate Immun* 2009; 1: 29–45.
 57. Tokunaga T, Yamamoto H, Shimada S, et al. Antitumor activity of deoxyribonucleic acid fraction from *Mycobacterium bovis* BCG. I. Isolation, physicochemical characterization, and antitumor activity. *J Natl Cancer Inst* 1984; 72: 955–962.
 58. Shimada S, Yano O, Inoue H, et al. Antitumor activity of the DNA fraction from *Mycobacterium bovis* BCG. II. Effects on various syngeneic mouse tumors. *J Natl Cancer Inst* 1985; 74: 681–688.
 59. Prins JM, Kuijper EJ, Mevissen ML, et al. Release of tumor necrosis factor alpha and interleukin 6 during antibiotic killing of *Escherichia coli* in whole blood: Influence of antibiotic class, antibiotic concentration, and presence of septic serum. *Infect Immun* 1995; 63: 2236–2242.
 60. Luo Y, Liu M, Dai Y, et al. Norisoboldine inhibits the production of pro-inflammatory cytokines in lipopolysaccharide-stimulated RAW 264.7 cells by down-regulating the activation of MAPKs but not NF- κ B. *Inflammation* 2010; 33: 389–397.
 61. Cooper A, Magram J, Ferrante J, et al. Interleukin 12 (IL-12) is crucial to the development of protective immunity in mice intravenously infected with *Mycobacterium tuberculosis*. 1997; 186: 39.
 62. Reiling N, Blumenthal A, Flad HD, et al. Mycobacteria-induced TNF- α and IL-10 formation by human macrophages is differentially regulated at the level of mitogen-activated protein kinase activity. *J Immunol* 2001; 167: 3339–3345.
 63. Xu G, Wang J, Gao GF, et al. Insights into battles between *Mycobacterium tuberculosis* and macrophages. *Protein Cell*. 2014; 5: 728–736.
 64. Jung SB, Yang CS, Lee JS, et al. The mycobacterial 38-kilodalton glycolipoprotein antigen activates the mitogen-activated protein kinase pathway and release of pro-inflammatory cytokines through Toll-like receptors 2 and 4 in human monocytes. *Infect Immun* 2006; 74: 2686–2696.
 65. Tino MJ and Wright JR. Surfactant protein A stimulates phagocytosis of specific pulmonary pathogens by alveolar macrophages. *Am J Physiol-Lung C* 1996; 4: 270.
 66. Underhill DM, Ozinsky A, Hajjar AM, et al. The Toll-like receptor 2 is recruited to macrophage phagosomes and discriminates between pathogens. *Nature* 1999; 401: 811–815.
 67. M. Bartl M, Luckenbach T, Bergner O, et al. Multiple receptors mediate apoJ-dependent clearance of cellular debris into nonprofessional phagocytes. 2001; 271: 130–141.
 68. Zhao AH, Kou LJ, Qiao LY, et al. preliminary study on immunological activity of BCG-CpG-DNA. *Chin J Biol* 2006; 19: 574–577.